DR1. (A) General petrographic description of samples

Hornblende andesite (samples A01 & D01)

The hornblende andesites are blue-grey rocks that consist of 40-50% medium to coarse phenocrysts in an aphanitic matrix (Fig. DR1-1). The phenocryst assemblage is composed mainly of oscillatory zoned plagioclase and hornblende (Figs. DR1-1, DR1-2) with minor olivine. The matrix also hosts abundant titanomagnetite and augite microphenocrysts. Plagioclase phenocrysts generally have a weak preferential alignment that is attributed to magma flow (Fig. DR1-2d,f). Hornblende phenocrysts are commonly large, reaching 15 mm (Fig. DR1-1a), can have patchy zoning (Figs. DR1-1d, DR1-2e) and are rimmed by fine-grained magnetite. Post-crystallisation alteration is limited to minor sericite replacement of plagioclase and green amphibole replacement of hornblende. The matrix also hosts aggregates of calcite and quartz (± apatite ± k-feldspar ± albite ± epidote) with highly resorbed boundaries (Fig. DR1-2g,h), which are interpreted to be remnants of crustal fragments (i.e., xenoliths) that were incorporated by the magma before or during eruption. Small zircon grains are found in association with these xenoliths, as described in a separate section below.

Basaltic andesite (samples D02 & D03)

The basaltic andesites resemble the hornblende andesites in grainsize and texture, but contain a much greater proportion of pyroxenes. They have a porphyritic texture (Figs. DR1-3, DR1-4) and the phenocryst assemblage is composed predominantly of large plagioclase (An_{70-55}), augite (Mg# 88-75), hornblende and olivine, with some orthopyroxene. Plagioclase, amphibole and titanomagnetite are the main constituents of the matrix, which is much coarser grained in sample D02 compared to D03. However, neither sample has a fine glassy groundmass as present in the hornblende andesites. Glomerophyric cluster of clinopyroxene, hornblende and magnetite that occur throughout the samples are interpreted to be accumulations of early-formed crystals. As with the hornblende andesite samples, both D02 and D03 preserve quartz-carbonate (± apatite ± k-feldspar ± albite ± epidote) xenoliths with resorbed grain boundaries (Fig. DR1-3g,h). Again, fine zircon grains may be associated with these xenoliths (see below). Alteration of the samples is limited to some serpentinisation of olivine, sericite replacement of plagioclase, thin carbonate veining, and epidote infilling of original vesicles.

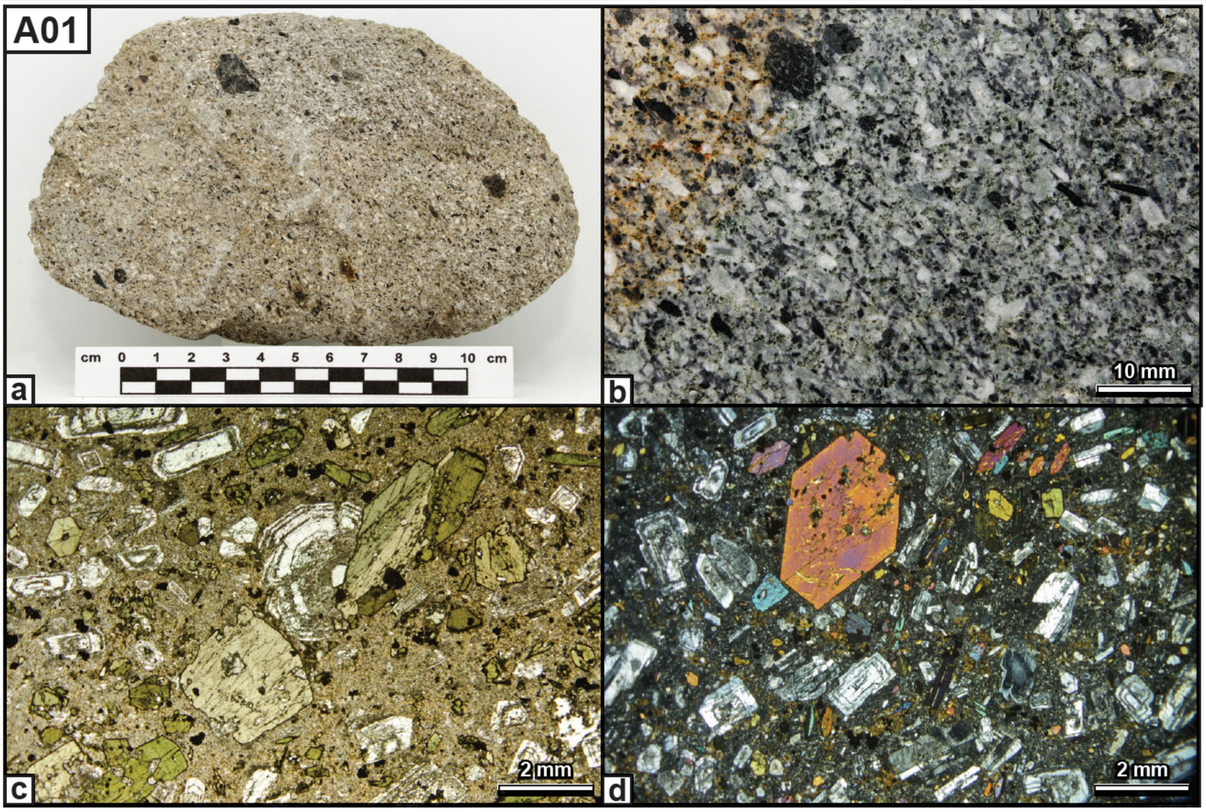

Figure DR1-1: a) Hornblende andesite sample A01 with coarse black hornblende phenocrysts evident. ***b)*** Cut surface showing yellow weathered rind and blue grey porphyritic texture of fresh rock. ***c)*** Plain polarised (PPL), and ***d)*** cross polarised photomicrographs with coarse hornblende phenocrysts (green in PPL, high birefringence in CPL), zoned plagioclase phenocrysts (white in PPL), titanomagnetite microphenocrysts (black) in an aphanitic matrix.

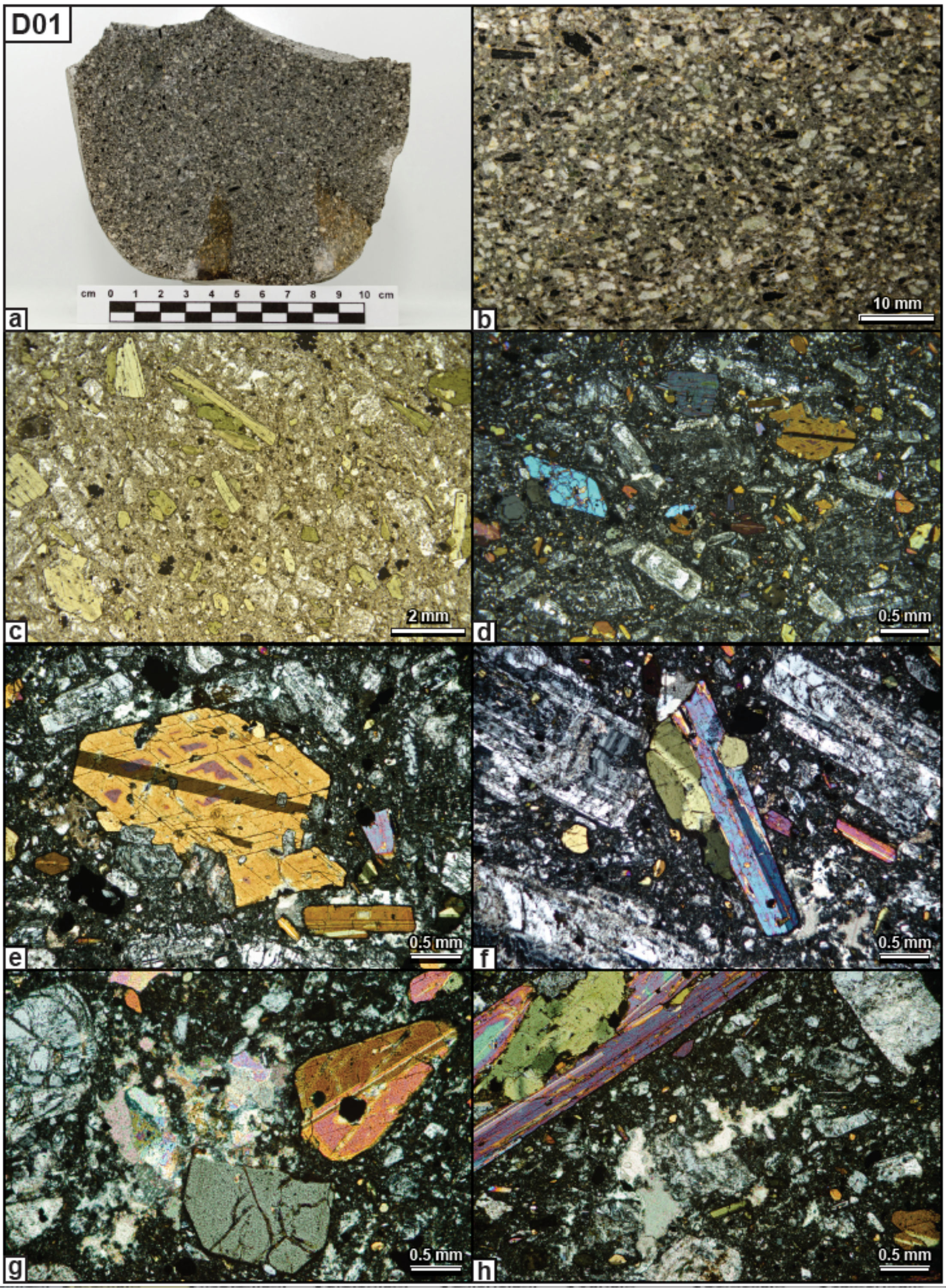

Figure DR1-2: a) Hornblende andesite sample D01. ***b)*** Cut surface showing the grey porphyritic texture of the fresh rock. ***c)*** Plain polarised (PPL), and ***d-h)*** cross polarised photomicrographs with coarse hornblende phenocrysts (green in PPL, high birefringence in CPL), zoned plagioclase phenocrysts (white in PPL), titanomagnetite phenocrysts (black) in an aphanitic matrix. Plagioclase phenocrysts commonly display oscillatory zoning and alignment. ***g, h)*** cross polarised photomicrographs of quartz carbonate xenoliths (centre of panel g, bottom centre of panel h) with irregular boundaries due to partial resorption by the host magma.

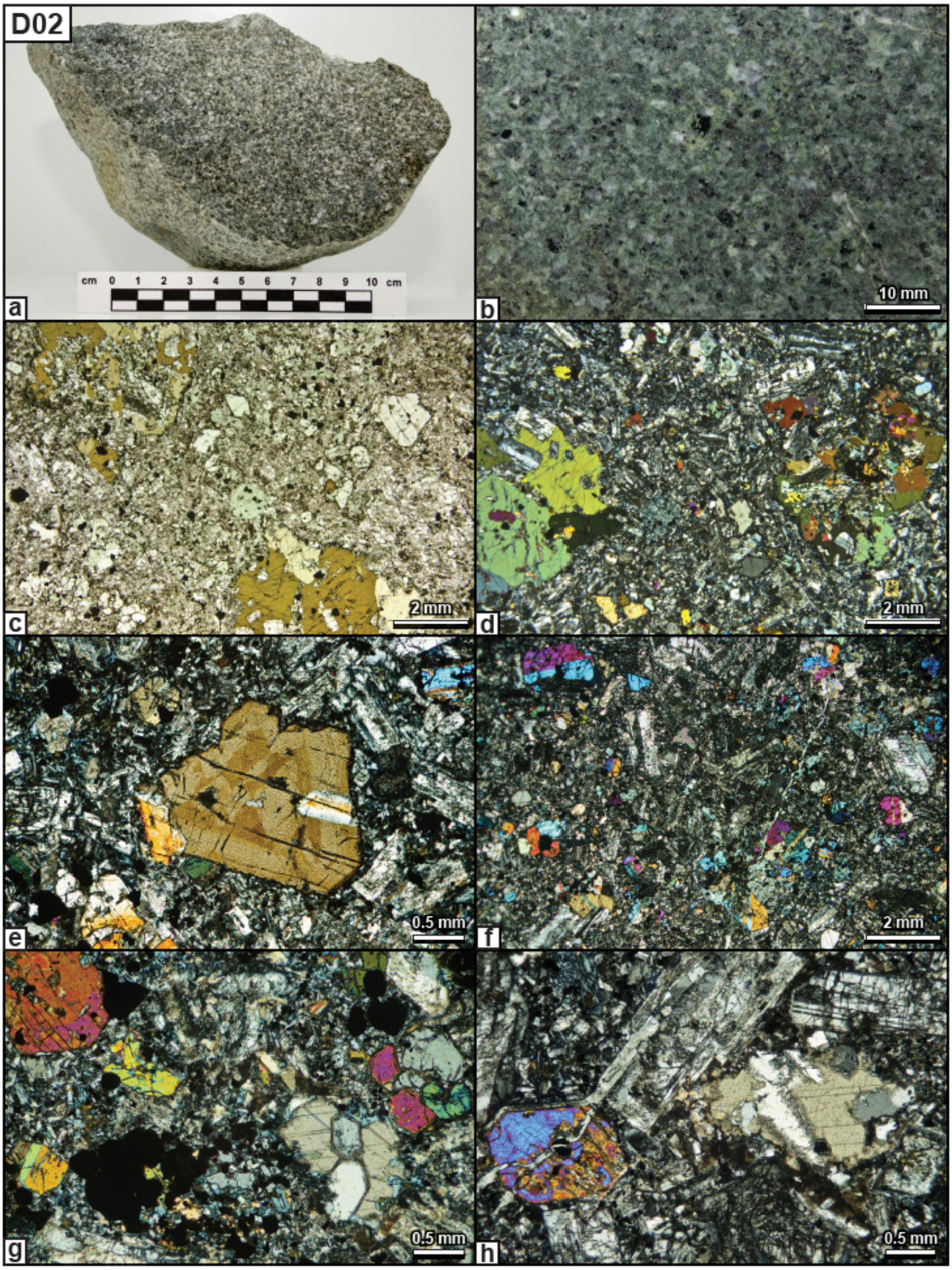

Figure DR1-3: a) Basaltic andesite sample D02. ***b)*** Cut surface showing the grey medium/coarse grained fresh rock with black hornblende phenocrysts and partially sericitised plagioclase (light green) ***c)*** Plain polarised (PPL), and ***d-h)*** cross polarised photomicrographs with coarse hornblende phenocrysts (olive brown in PPL, high birefringence in CPL), tabular plagioclase phenocrysts (white in PPL), and augite (light green in PPL) in a medium grainsize matrix. Hornblende phenocrysts often preserve patchy zonation ***(e)***. ***g, h)*** cross polarised photomicrographs of quartz carbonate xenoliths (bottom right of panel g, centre right of panel h) with irregular boundaries due to partial resorption by the host magma.

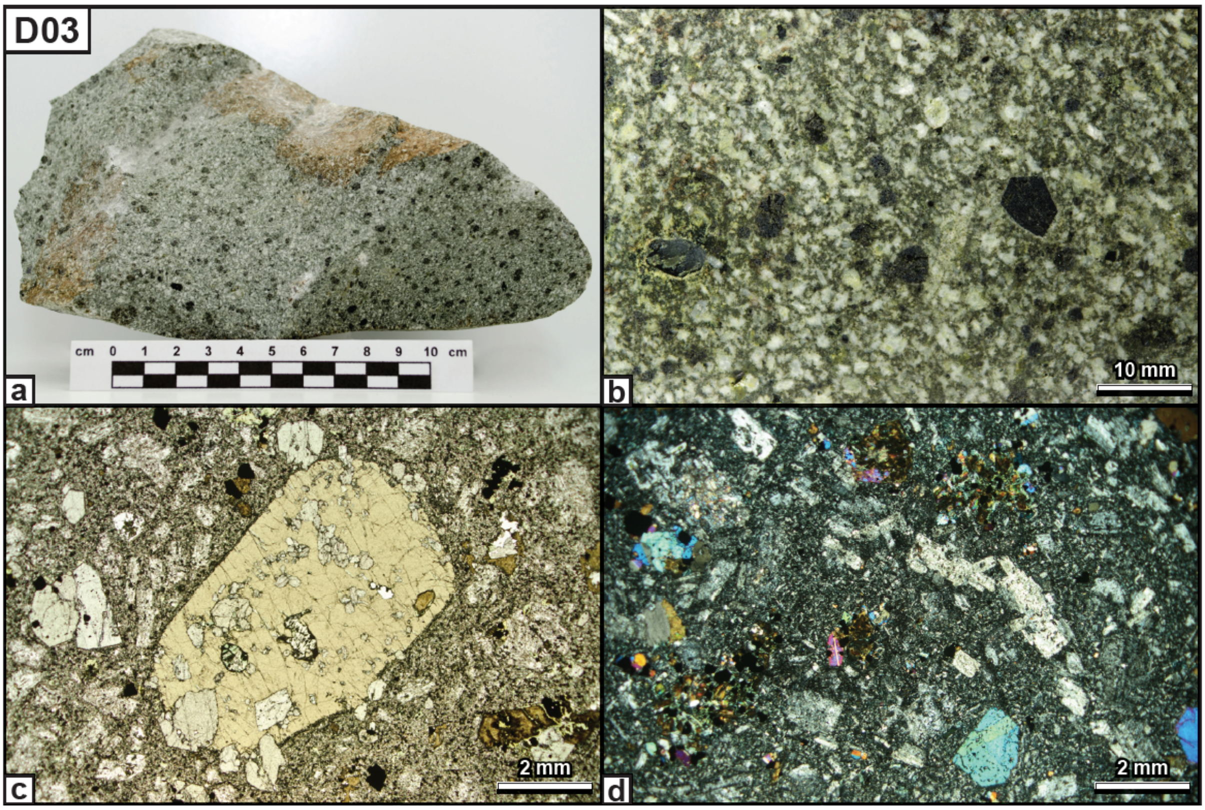

Figure DR1-4: a) Basaltic andesite sample D03. ***b)*** Cut surface showing the grey porphyritic texture with coarse black hornblende phenocrysts and medium-grained plagioclase phenocrysts ***c)*** Plain polarised (PPL), and ***d)*** cross polarised photomicrographs with coarse hornblende phenocrysts (yellow-brown in PPL, high birefringence in CPL), plagioclase phenocrysts (white in PPL), and augite (light green in PPL) and black titanomagnetite in a fine-grained matrix.

Dolerite (sample BTM4)

Sample BTM4 is the most mafic rock of the sample suite. The rock has a porphyritic texture with phenocrysts of plagioclase, clinopyroxene and hornblende set in a medium grained, partially altered groundmass of amphibole, plagioclase and magnetite (Fig. DR1-5). Relatively low temperature alteration is expressed by infilling of vesicles by zeolites (probably laumontite) and Fe oxides, partial sericite alteration of plagioclase, and dissemination of secondary pyrite throughout the rock.

Sample BTM4 contains various cumulate and xenolithic inclusions. Most notable are gabbroic cumulate blocks ranging between 15 and 20 mm in diameter (Fig. DR1-5e,f) that are composed of granular clinopyroxene, orthopyroxene, hornblende, altered plagioclase and magnetite. Other cumulate inclusions consist only of clusters of pyroxene and spinel. Quartz carbonate crustal xenoliths are occasionally observed, but these are less common here than in the hornblende andesites and basaltic andesites.

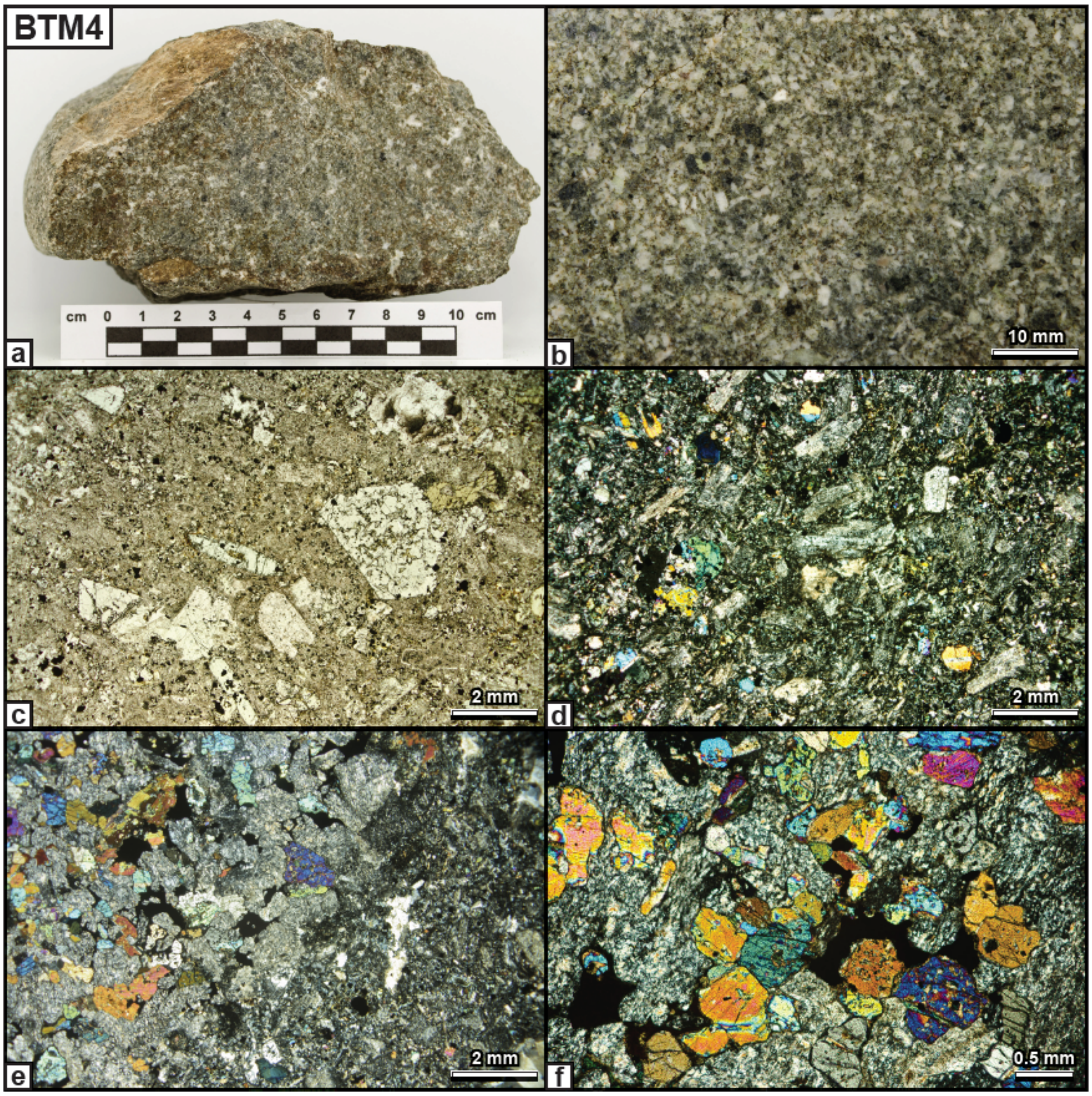

Figure DR1-5: a) Dolerite sample BTM4. ***b)*** Cut surface showing the grey medium/coarse grained fresh rock with black hornblende, grey/green pyroxene and white plagioclase phenocrysts ***c)*** Plain polarised (PPL), and ***d-f)*** cross polarised photomicrographs with augite (light green in PPL) and plagioclase phenocrysts (white in PPL), in a medium grainsize matrix. ***e, f)*** Coarse gabbroic xenoliths (left side of panel e) consisting of pyroxenes, altered plagioclase and magnetite.

Tonalite (sample D04)

Sample D04 is the only plutonic rock in the sample suite. It is a coarse-grained phaneritic rock largely composed of zoned plagioclase (~70%), with minor quartz (~10%), hornblende and magnetite (Fig. DR1-6). The hornblende is extensively altered to chlorite and calcite (Fig. DR1-6d), and secondary pyrite is common. Accessory phases include titanite, apatite and disseminated zircon. Plagioclase is nearly free of alteration and displays complex zonation patterns (including oscillatory, continuous and patchy zonation; Fig. DR1-6c,d), which is indicative of the complex crystallisation history of this rock.

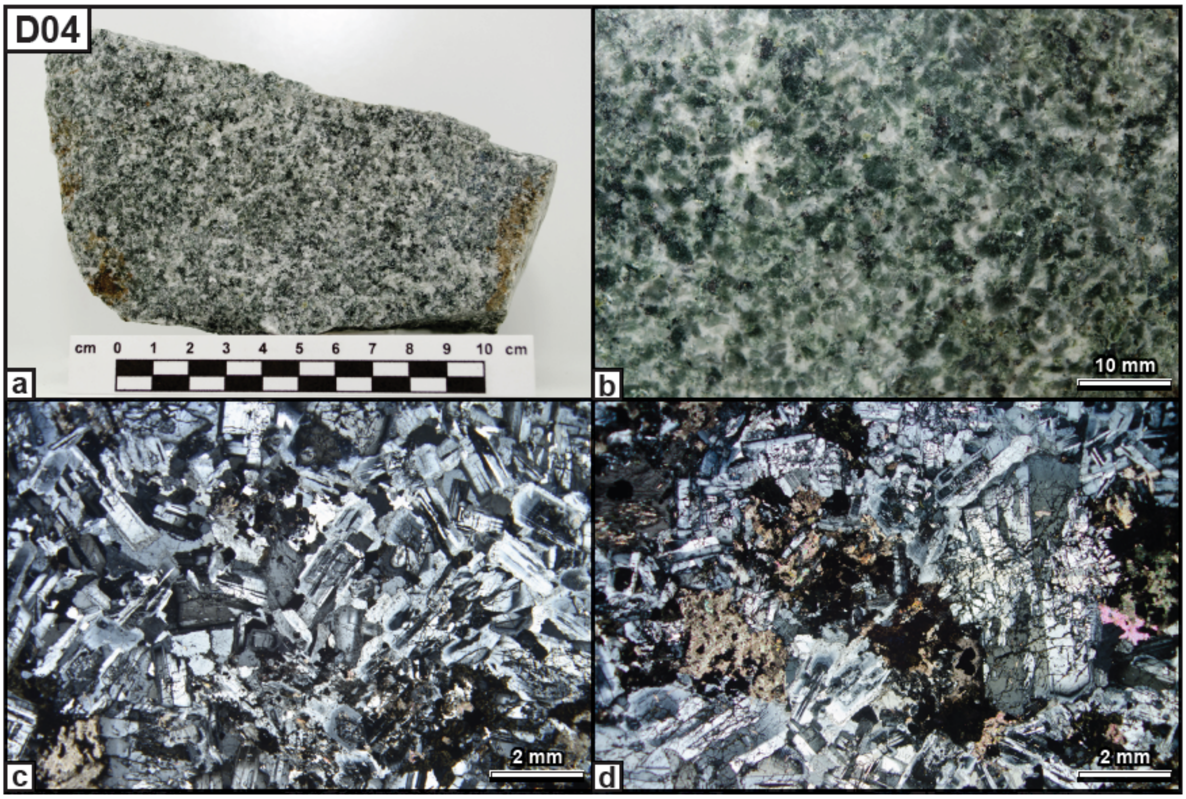

Figure DR1-6: a) Tonalite sample D04. ***b)*** Cut surface showing the grey coarse grained phaneritic texture of the rock. ***c, d)*** Cross polarised photomicrographs with complexly zoned interlocking plagioclase grains and hornblende altered to chlorite and calcite (high birefringence phases).

DR1. (B) Petrographic description of zircon in the Santo volcanic rock samples

A relatively high yield of zircon grains were recovered following heavy mineral separation procedures of samples D01, D02 and D03 (see DR4), despite the fact that zircon grains were not observed during petrographic study of thin sections of these rocks. However, the following simple mass balance calculation demonstrates that this result is to be expected. Consider;

1. Between 3 and 4 kg of each sample was processed for zircon separation. We will use a figure of 3 kg for the calculation.
2. Less than 100 grains were hand-picked for each separation procedure. Clearly, more grains are present in the sample, so we assume a yield of 1000 grains (i.e., 10 times the number hand-picked) for the calculation.
3. Zircon grains of variable size were separated, with the largest reaching several hundred μm in length (see DR5). For the calculation we assume generous dimensions of 200 μm x 100 μm x 100 μm for all grains.
4. Using these figures (and a zircon specific gravity of 4.6), the zircon yield amounts to **3.1 ppm of zircon in the rock**. Given that zircon contains ~43% zirconium, this equates to less than 1.5 ppm (or less than 2%) of the bulk rock Zr content (which is between 71 and 82 ppm; see DR2).

Considering these figures, attempting to find large zircon grains in situ (i.e., in thin section) can be considered to be a "needle-in-a-haystack" type exercise. Nevertheless, in an effort to understand the textural context of the zircon grains in the rock samples, we undertook additional petrographic analysis of these samples by X-ray mapping and backscattered electron imaging using a JEOL JXA8200 superprobe, housed at the Advanced

Analytical Centre, James Cook University. To find zircon grains in the sections, we employed a scanning X-ray technique similar to that outlined by Sack et al. (2011). We acquired Zr (+ Si, K, Ca, Fe) x-ray maps of polished rock sections using a 15 kV, 100 nA electron beam defocussed to 40 µm. Maps were set up with a 40 µm step with counting times of 100 to 120 milliseconds per step. Interrogation of the resulting maps showed that the technique could be used to find sub-µm sized zircon grains. Examples of the X-ray maps are given below in Fig. DR1-7. EDS analysis was used for mineral identification.

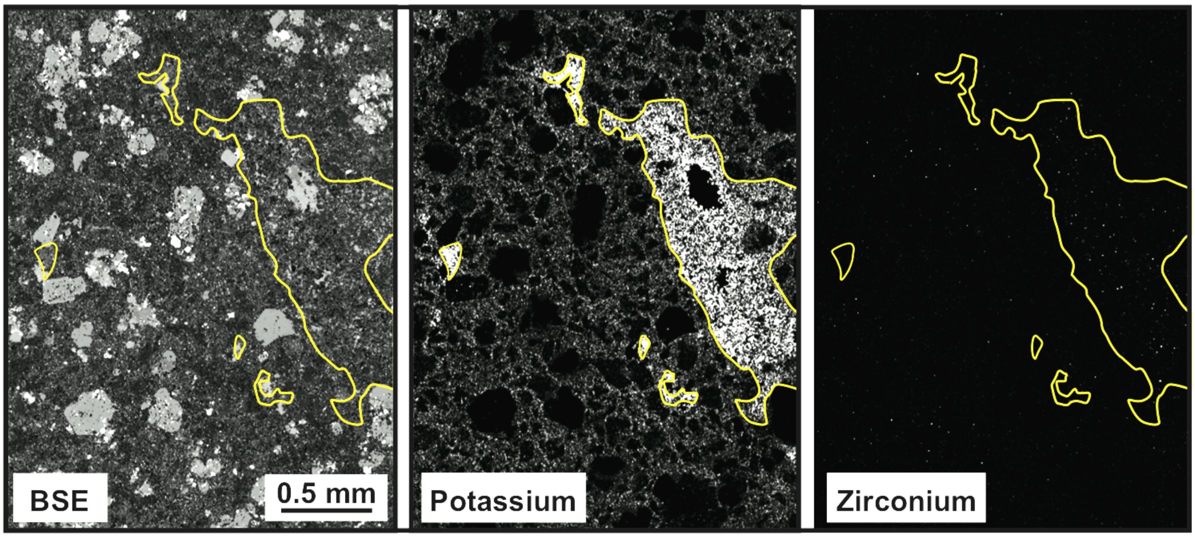

Figure DR1-7: Backscattered electron (BSE) image and potassium and zirconium x-ray maps of basaltic andesite sample D03. The bright white and light grey phases in the BSE image are magnetite and hornblende grains, respectively. The high K zones outlined in yellow correspond to partially dissagregated crustal xenoliths. Pixels recording high Zr counts mostly correspond to small (0.5 – 5 µm) zircon grains. Note the relatively high concentration of zircon grains in the xenolith.

Zircon grains were discovered in all sections analysed (7 x D01, 1 x D02, 1 x D03), but all of the zircon grains were less than 15 µm in size, which is too small for in-situ U-Pb age dating (see DR4 and Sack et al., 2011). Nevertheless, we were able to: 1. Demonstrate that zircon grains are indeed present in these rocks, and: 2. Document the textural setting and petrogenetic context of the zircon grains. In some cases, fine zircon grains appeared to be loosely held in cracks and cavities in the sections. These grains may be contamination from polishing procedures (e.g., see Dobrzhinetskaya et al., 2014) and hence were not further considered. In other cases, zircon grains are enclosed within quartz or calcite grains, or within hornblende phenocrysts and so are not considered to be artefacts of sample preparation procedures. We identify two primary textural associations of these zircon grains. 1. Most zircon grains are found in association with partially disaggregated xenoliths composed of quartz with or without calcite, K-feldspar, albite, epidote, apatite and trace titanite (Fig. DR1-7 and 8). Most xenolith grains preserve evidence of partial digestion/resorption by the host magma. The carbonate-bearing xenoliths are interpreted to be of sedimentary or metamorphic origin, whereas feldspar-bearing, carbonate-free xenoliths may be igneous in origin. The zircon grains may have irregular or highly corroded grain boundaries (Fig. DR1-8e,f), which is consistent with partial resorption by the magma, or they may preserve euhedral forms (Fig. DR1-8a) indicating the grains remained shielded from the magma inside xenolith minerals such as quartz or calcite.

The second textural setting for zircon grains is as euhedral inclusions within hornblende phenocrysts (Fig. DR1-8g,h). These zircons are associated with apatite inclusions, and are interpreted to derive from crustal material that was assimilated during phenocryst growth at a relatively early (deeper) stage of magma evolution.

The two textural settings and variable forms of zircon in these rocks provide evidence that there were multiple stages of assimilation (or continuous assimilation) of crustal material during storage and migration of magma in the arc crust. These observations also provide an explanation for the range of zircon grain morphologies recovered from mineral separation procedures (DR5) and in part may explain the diversity of ages of the zircon record.

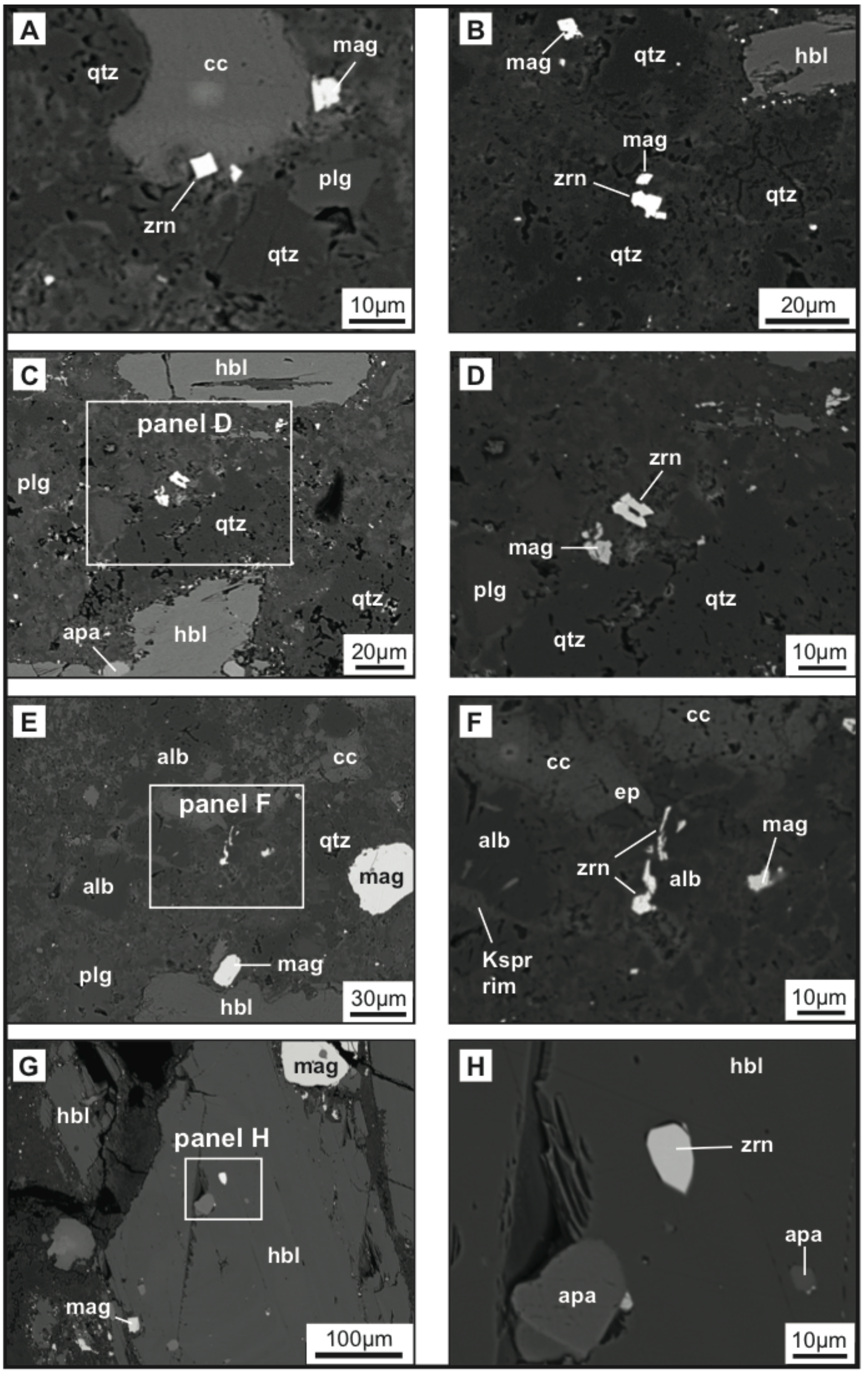

Figure DR1-8: Backscattered electron (BSE) images of zircon grains in hornblende andesite sample D01. ***(a)*** Euhedral zircon sitting within calcite in a quartz-calcite dominated xenolith. ***(b)*** Cluster of small subhedral zircon grains within quartz of a partially-disaggregated quartz-rich xenolith. ***(c, d)*** Subhedral zircon grains associated with a partially-disaggregated quartz-rich xenolith. ***(e, f)*** Anhedral zircon grain associated with a partially-disaggregated xenolith of calcite, albite, K-feldspar and epidote. The zircon and other xenolith grains preserve evidence of partial resorption by the host magma. Note the corroded boundaries of the hornblende and magnetite phenocrysts in ***(c)*** and ***(e)***. ***(g, h)*** Euhedral zircon inclusion associated with apatite inclusions in a large hornblende phenocryst. Mineral abbreviations: alb = albite, apa = apatite, cc = calcite, ep = epidote, hbl = hornblende, Kspr = K-feldspar, mag = magnetite, plg = plagioclase, qtz = quartz, zrn = zircon.

References:

Dobrzhinetskaya, L., Wirth, R., and Green, H., 2014, Diamonds in Earth's oldest zircons from Jack Hills conglomerate, Australia, are contamination. Earth and Planetary Science Letters, v. 387, p. 212-218.

Sack, P.J., Berry, R.F., Meffre, S., Falloon, T.J., Gemmell, J.B., and Friedman, R.M., 2011, In situ location and U-Pb dating of small zircon grains in igneous rocks using laser ablation-inductively coupled plasma-quadrupole mass spectrometry. Geochemistry, Geophysics, Geosystems, v. 12, Q0AA14, doi: 10.1029/2010GC003405.

DR2. Bulk rock geochemical and Sr-Nd isotope composition of Santo igneous rocks, and calculations of mixing of continental crust and basalt using Nd isotopes

Analytical methods

The rock samples (~3 to 4 kg) were initially processed using a hydraulic splitter to remove weathered surfaces and fractures. The samples were then crushed to chips in a tungsten carbide plate crusher, and a representative portion of chips milled to a fine powder in a tungsten-carbide ring mill. Rigorous cleaning of all equipment between sample processing was implemented to avoid cross contamination between samples.

The powders were used to produce fusion glass beads with 12:22 Li-borate flux from which major and trace elements were respectively determined by conventional XRF using a Bruker-ASX S4 Pioneer XRF, and laser ablation ICP-MS using a Geolas Pro 193 nm ArF excimer laser coupled with a Bruker 820-MS ICP-MS at the Advanced Analytical Centre, James Cook University (JCU). Details of the analytical set-up and data reduction are presented in Holm et al. (2013).

Sm-Nd and Sr isotopes were determined from digested powdered rock samples (in PARR acid digestion bombs) at the University of Adelaide with a Finnigan MAT262 thermal ionization mass spectrometer (TIMS), in static and quadruple cup dynamic measurement modes following the routine described in Wade et al. (2006). The measurements were corrected for mass fractionation by normalization of $^{88}Sr/^{86}Sr$ to 8.375209 and $^{146}Nd/^{144}Nd$ to 0.7219. Reference materials JNdi-1 and SRM987 were 0.512081 ± 12 (2SD) (n=4), and 0.710263 ± 13 (2SD) (n=8), respectively. Whole rock $^{143}Nd/^{144}Nd$ ratios were normalised to the TIMS value of JNdi-1 (0.512098 ± 13; Fisher et al., 2011). The geochemical and isotopic data are tabulated in Table DR2.

Table DR2. Bulk-rock geochemical and Sr-Nd isotope composition of Santo igneous rocks

Sample	**A01**	**BTM4**	**D01**	**D02**	**D03**	**D04**
rock-type	hble andesite	dolerite	hble andesite	basaltic andesite	basaltic andesite	tonalite
Major elements (wt.%)						
SiO_2	62.23	50.72	57.94	52.45	53.12	53.36
TiO_2	0.61	0.94	0.60	0.82	0.80	0.79
Al_2O_3	16.18	17.14	16.96	17.72	18.24	20.53
Fe_2O_3	6.10	8.97	6.63	8.66	8.22	5.98
MnO	0.10	0.20	0.16	0.18	0.17	0.12
MgO	2.58	4.29	2.53	4.17	3.52	2.16
CaO	5.67	7.05	5.37	8.54	6.39	8.52
Na_2O	4.36	4.56	4.46	3.20	4.97	4.09
K_2O	0.33	1.17	2.07	0.86	1.56	0.29
P_2O_5	0.17	0.18	0.18	0.13	0.20	0.30
LOI	1.81	4.80	3.11	3.31	2.71	3.64
total	100.14	100.02	100.01	100.04	99.90	99.78
trace elements (ppm)						
Sc	12.7	24	10.3	22	17.7	9.5
Ti	3660	5640	3600	4920	4740	4740
V	158	279	164	229	209	148
Cr	23	51	18	47	35	20
Ni	13	21	5.4	27	15.5	8.4
Cu	14	69	25	36	28	10
Zn	22	86	56	73	70	65
Rb	5.79	15.8	24.6	13.2	28.1	1.82
Sr	294	417	390	342	490	608
Y	17.1	18.7	18.7	20.7	21.4	22.5
Zr	73.7	74.1	79.6	71.6	81.6	83.2
Nb	3.27	4.03	4.22	2.28	2.97	3.18
Cs	0.07	0.13	0.14	0.23	0.47	0.21
Ba	101	240	426	181	218	126
La	12.9	13.8	16.1	18.8	10.9	18.5
Ce	20.8	23.3	27.9	17.2	22.2	25.0
Pr	2.71	2.88	3.44	2.27	2.92	3.19
Nd	11.4	13.1	14.8	11.2	13.9	15.4
Sm	2.68	3.17	3.11	2.89	3.10	3.69
Eu	0.85	1.00	1.01	0.96	1.05	1.22
Gd	2.97	3.18	3.02	3.37	3.45	4.02
Tb	0.44	0.51	0.46	0.52	0.56	0.61
Dy	2.98	3.37	3.25	3.69	3.78	4.08
Ho	0.62	0.67	0.66	0.73	0.79	0.83
Er	1.91	2.12	1.90	2.35	2.39	2.60
Yb	1.94	1.96	2.00	2.21	2.33	2.42
Lu	0.29	0.30	0.31	0.35	0.38	0.40
Hf	2.03	2.12	2.26	2.12	2.22	2.50
Pb	1.85	4.56	3.02	2.38	1.81	2.07
Th	1.65	1.46	2.45	1.20	1.47	1.95
U	0.58	0.55	0.79	0.47	0.60	0.56
$^{87}Sr/^{86}Sr^{i}$	0.703545	0.704794	0.703869	0.703763	0.704236	nd
$^{143}Nd/^{144}Nd^{i}$	0.512953	0.512964	0.512957	0.512960	0.512946	nd

Notes: nd = no data. hble = hornblende. Sr and Nd istope values calculated to initial age of the rock.

Neodymium isotope calculations of continental crust assimilation by basalt

We have employed a Nd isotope mixing model to determine how much assimilation of continental crust by a mid-ocean-ridge basalt (MORB; representing a mantle melt unmodified by subduction components) would be required to derive the Nd isotope composition of the Santo volcanic rocks. Using the age distribution of inherited zircons from Vanuatu as shown in Figure 1, and the Sm-Nd isotope composition of representative Australian crust through time from Allègre and Rousseau (1984), we calculate a $^{143}Nd/^{144}Nd$ isotope composition and Nd concentration for the bulk continental crust present within Vanuatu of 0.511380 and 29 ppm, respectively. For the MORB end-member of the mixing calculations we use the $^{143}Nd/^{144}Nd$ and Nd concentration of MORB from Kelemen et al. (2003) of 0.51310 and 9.3 ppm, respectively. These values are fairly typical of normal and depleted MORB globally (e.g., see Jenner and O'Neill, 2012, and http://earthref.org/GERMRD/e:60/).

Mixing about 3% of the continental crust end-member with ~97% MORB can reproduce the average $^{143}Nd/^{144}Nd$ of the Santo volcanic rocks (0.512956). This level of crustal assimilation would not markedly change the major element composition of the volcanic rock, and would be consistent with the petrographic observation of inherited zircons and crustal xenoliths in the Santo volcanic rocks. However, mixing 3% upper continental crust (composition taken from Rudnick and Gao, 2003) with MORB (from Sun and McDonough, 1989) cannot reproduce the trace element characteristics of the Santo igneous rocks, as shown in Figure 2 in the manuscript.

References:

Allègre, C. J., and Rousseau, D., 1984, The growth of the continent through geological time studied by Nd isotope analysis of shales. Earth and Planetary Sciences Letters, v. 67, p. 19-34.

Fisher, C. M., McFarlane, C. R. M., Hanchar, J. M., Schmitz, M. D., Sylvester, P. J., Lam, R., and Longerich, H. P., 2011, Sm–Nd isotope systematics by laser ablation-multicollector-inductively coupled mass spectrometry: Methods and potential natural and synthetic reference materials. Chemical Geology, v. 284, p. 1–20.

Holm, R. J., Spandler, C., and Richards, S. W., 2013, Melanesian arc far-field response to collision of the Ontong Java Plateau: Geochronology and petrogenesis of the Simuku Igneous Complex, New Britain, Papua New Guinea. Tectonophysics, v. 603, p. 189-212.

Kelemen, P. B., Hanghøj, K., and Greene, A. R., 2003, One view of the geochemistry of subduction-related magmatic arcs, with an emphasis on primitive andesite and lower crust. Treatise on Geochemistry, v. 3, p. 593-659.

Jenner, F. E., and O'Neill, H. St. C., 2012, Analysis of 60 elements in 616 ocean floor basaltic glasses. Geochemistry Geophysics Geosystems, v. 13, Q02005.

Rudnick, R. L., and Gao, S., 2003, Composition of the continental crust. Treatise on Geochemistry, v. 3, p. 1-64.

Sun, S. S., and McDonough, W. F., 1989, Chemical and isotopic systematics of oceanic basalts; implications for mantle composition and processes. In: Saunders, A. D., and Norry, M. J., eds., Magmatism in the ocean basins. Geological Society of London Special Publications, v. 42, p. 313-345.ßß

Wade, B. P., Barovich, K. M., Hand, M., Scrimgeour, I. R., and Close, D. F., 2006, Evidence for early Mesoproterozoic arc magmatism in the Musgrave Block, central Australia: implications for Proterozoic crustal growth and tectonic reconstructions of Australia. Journal of Geology, v. 114, p. 43-63.

DR3. Analytical methods and results of Ar-Ar dating of hornblende from Santo volcanic rocks

Analytical methods

Pristine hornblende phenocrysts were hand picked from three coarsely crushed volcanic rocks samples. The grain separates were cleaned in an ultrasonic bath and were wrapped in pure Al foil and irradiated for 90 MWhr at location 8E at the McMaster Nuclear Reactor at McMaster University in Hamilton, Ontario in irradiation package mc41. Standard hornblende MMhb-1 was used as a neutron fluence monitor with an assumed age of 520.4 Ma (Samson and Alexander, 1987). All samples were incrementally heated with a Coherent Innova 5 W continuous argon-ion laser until complete fusion was achieved. For each degassing step, the system was programmed to heat each grain in turn for 30 seconds. Ar isotopes were measured using a VG1200S mass spectrometer with a source operating at 150 mA total emission and equipped with a Daly detector operating in analog mode. Mass discrimination was monitored daily using ~4×10^{-9} ccSTP of atmospheric Ar. Fusion system blanks were run every five fusion steps and blank levels from argon masses 36 through 40 (~2×10^{-14}, ~3×10^{-14}, ~1×10^{-14}, ~3×10^{-14}, and 2×10^{-12} ccSTP respectively) were subtracted from sample gas fractions. Corrections were also made for the decay of ^{37}Ar and ^{39}Ar, as well as interfering nucleogenic reactions from K, Ca and Cl as well as the production of ^{36}Ar from the decay of ^{36}Cl. The Ar-Ar age data are presented in Table DR3.

References:

Samson, S. D., and Alexander, E. C., 1987, Calibration of the interlaboratory $^{40}Ar/^{39}Ar$ dating standard, Mmhb-1. Chemical Geology, v. 66, p 27-34.

Table DR3. Ar-Ar age data for hornblende from Santo volcanic rocks

sample	A01	D01	D03
rock type	hornblende andesite	hornblende andesite	basaltic andesite
plateau age (Ma)	15.88 ± 0.35	18.36 ± 0.38	35.4 ± 3.8
MSWD	*0.56*	*0.48*	*1.07*
isochron age (Ma)	16.17 ± 0.34	18.53 ± 0.41	35.5 ± 5.2
MSWD	*0.97*	*0.53*	*0.92*
n	*39*	*26*	*26*

D01 hornblende

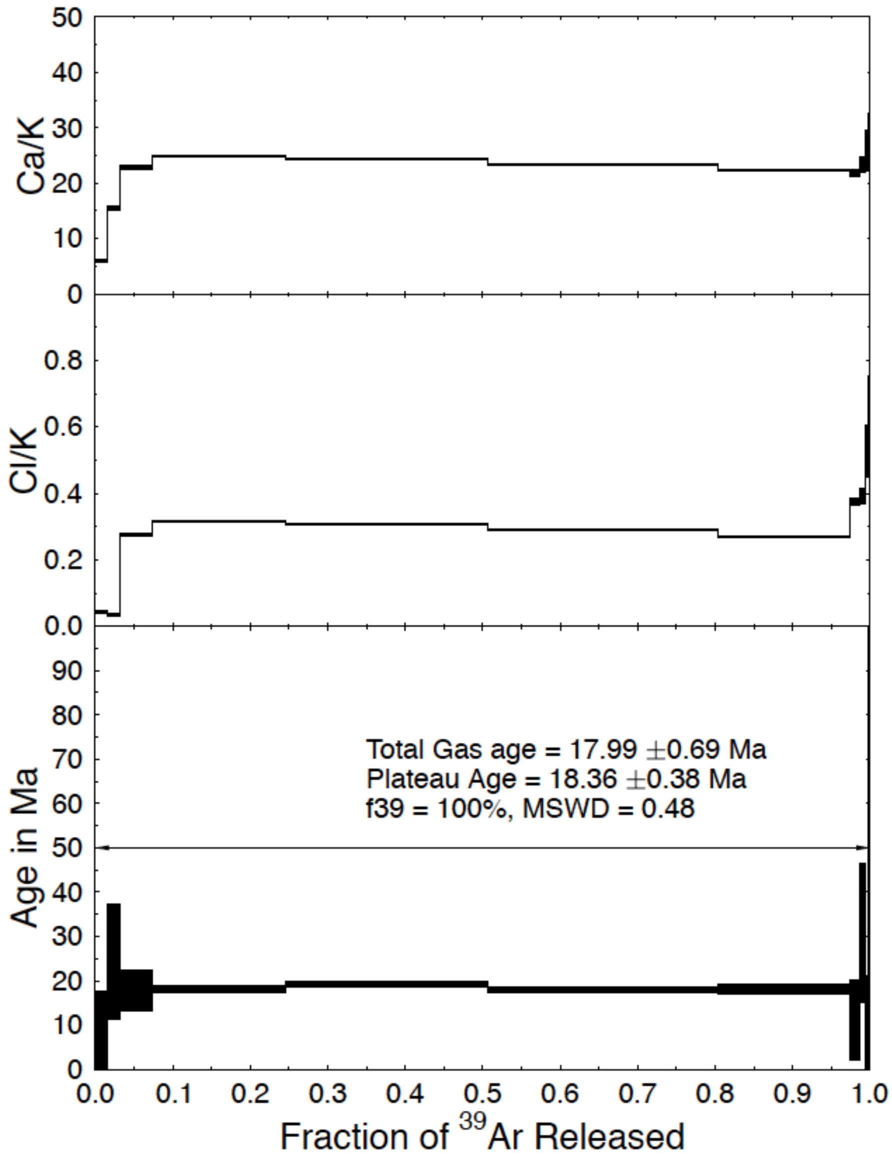

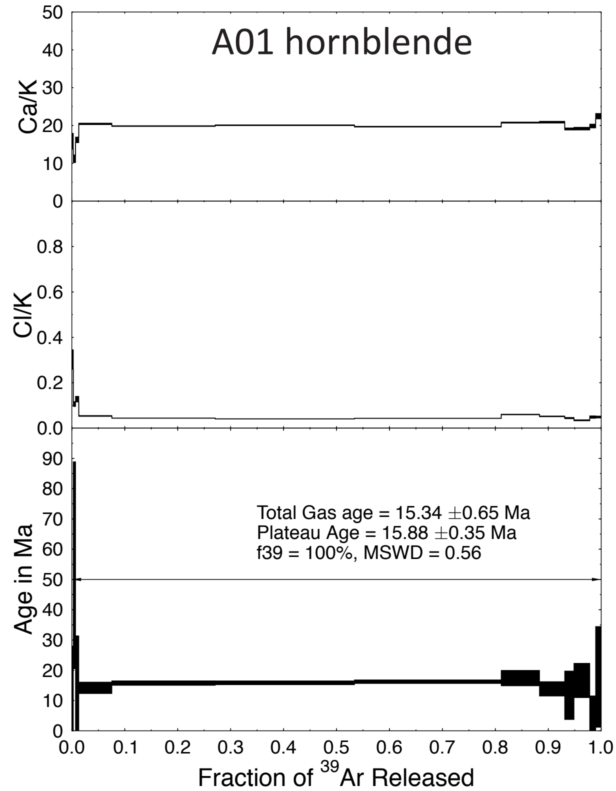
A01 hornblende
Ca/K
Cl/K
Age in Ma
Total Gas age = 15.34 ±0.65 Ma
Plateau Age = 15.88 ±0.35 Ma
f39 = 100%, MSWD = 0.56
Fraction of 39Ar Released

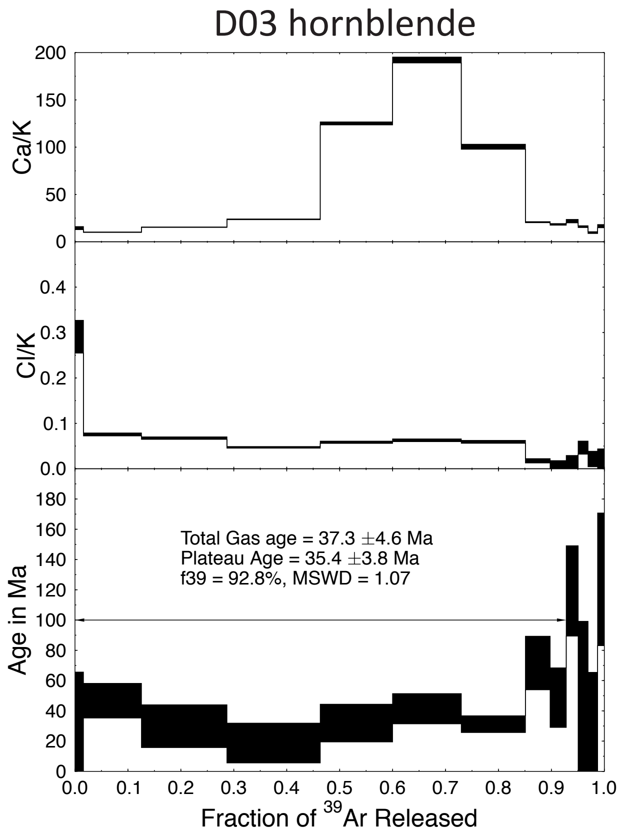
D03 hornblende
Ca/K
Cl/K
Age in Ma
Total Gas age = 37.3 ±4.6 Ma
Plateau Age = 35.4 ±3.8 Ma
f39 = 92.8%, MSWD = 1.07
Fraction of 39Ar Released

DR4. U-Pb dating methods and results

Mineral separation procedures and the issue of laboratory contamination

Mineral separation was carried out at James Cook University (JCU) in a standard four-step process similar to that described by Tucker et al. (2013). Samples were crushed and milled to 500 μm, washed to remove the clay-size fraction, and separated by a combination of heavy liquid density separation and magnetic separation. Care was taken to ensure all equipment was thoroughly cleaned before and after use to minimize the potential of any cross sample contamination. All zircons within the separates were hand picked and mounted in epoxy with GJ1, FC1, Temora 2 and Fish Canyon Tuff zircon standards. Epoxy mounts were then polished and carbon-coated.

Given the unexpected distribution of zircon ages from the volcanic rocks (Fig. 3), we were especially wary of the possibility of sample contamination during mineral processing and polishing procedures (e.g., Dobrzhinetskaya et al., 2014). Therefore, we undertook two separate and independent sample processing routines for the two samples with the highest zircon yields (D01 and D02) to check for possible sample contamination during processing. In all cases, the age distributions of zircons recovered (total of 280 pre-Eocene grains; Table DR4-2) from each separation routine (7 independent separations on 5 samples: Table DR4-2) were consistent. We also highlight a number of key points that confirm that our results are not an artifact of sample contamination.

1. At the time of sample processing, our mineral separation laboratory had only been in in operation for about two years. Much of the equipment was less than two years old. Strict protocols for lab use were (and are) imposed (e.g., the lab remains locked

when not in use, only one sample is processed at any time, lab users undertake thorough cleaning of equipment and lab surfaces before and after sample processing). Significant cross sample contamination has never been observed in samples processed using the same procedures employed here. For example, all 36 analyses of zircon from our tonalite sample D04 returned ages within tight uncertainty of 16.7 Ma (Table DR4-1; Fig, DR4-2). This sample was processed in the same way and at the same time period as our volcanic rock samples and clearly has not suffered from sample contamination.

2. Samples with Paleoproterozoic (1.8-2.0 Ga) and Rodinia break-up age (850-700 Ma) zircon populations were never processed in our laboratory prior to the samples from Santo. Therefore, we can categorically rule out sample contamination as the source of zircons of these ages in the Santo samples. These two age groups collective account for 43% of the total pre-Eocene zircon population of our samples (Fig. 1).

3. Zircon grains have been documented in situ in samples D01, D02 and D03 (see DR1-B). Although the observed grains were too small for in situ age dating, they do occur in association with crustal xenoliths that were in various stages of assimilation by the host magma at the time of eruption, or as inclusions inside igneous phenocrysts (DR1-B). The variety of xenolith types and textural settings of the zircons is consistent with assimilation and incorporation of a range of crustal lithologies over a protracted magmatic history, which may in part account the vast age distribution of zircons recovered from the mineral separation procedures.

Considering the laboratory protocols employed and the points outlined above, we find it implausible that the vast number and spectrum of ages of zircons found in the Santo volcanic rock samples is a result of laboratory contamination.

Analytical techniques and data processing

All analytical work was completed at the Advanced Analytical Centre, JCU. Cathodoluminescence (CL) images of all zircon crystals were obtained using a JEOL JSM5410LV scanning electron microscope equipped with a Robinson CL detector. Examples of the CL images are presented in Data Repository DR5. U-Pb dating of zircon was conducted using laser ablation ICP-MS, as described in Tucker et al. (2013). Analytes collected were ^{29}Si, ^{90}Zr, ^{202}Hg, ^{204}Pb, ^{206}Pb, ^{207}Pb, ^{208}Pb, ^{232}Th, ^{235}U, and ^{238}U. The ICP-MS was tuned to ensure low oxide production levels (ThO/Th <0.5%) and approximately equal sensitivity of U, Th and Pb to minimize isotope fractionation due to matrix effects. Fractionation and mass bias was corrected by using standard bracketing techniques with every ten zircon sample measurements bracketed by measurements of GJ1 (primary calibration standard; Jackson et al., 2004), Temora 2 (Black et al., 2004), Fish Canyon Tuff (Schmitz and Bowring, 2001; Renne et al., 2010) and FC1 (Orihashi et al., 2008). All zircons were analyzed with a beam spot diameter of 24 µm and selection of analytical sample spots was guided by CL images targeting both cores and rims. Analysis of the NIST SRM 612 reference glass was conducted at the beginning, middle and end of every analytical session.

Data reduction was carried out using the Glitter software (Van Achterbergh et al., 2001). All time-resolved single isotope signals from standards and samples were filtered for signal spikes or perturbations related to inclusions and fractures. Subsequently, the most stable and representative isotopic ratios were selected taking into account possible mixing of different age domains and zoning. Drift in instrumental measurements was corrected following analysis of drift trends in the raw data using measured values for the GJ1 primary zircon standard. Analyses of the secondary zircon standards were used for verification of GJ1 following drift correction. Age calculations for Temora 2, FC1 and Fish Canyon Tuff zircon standards were 419.3 ± 2.4 Ma, 1106 ± 12 Ma, and 28.39 ± 0.25 Ma, respectively (Fig. DR5-1), which compare well with published values of 416.8 Ma for Temora 2 (Black et al., 2004), 1111 Ma for FC1 (Orihashi et al., 2008) and 28.40 Ma for Fish Canyon Tuff zircon (Schmitz and Bowring, 2001).

Age reduction of primary magmatic zircons utilized Tera-Wasserburg Concordia plots (Tera and Wasserburg, 1972; Jackson et al., 2004) to account for the effects of common Pb and was carried out using Isoplot/Ex version 4.15 (Ludwig, 2009). Uncertainty was propagated and reported at 2σ level. All data are presented in Table DR4-1. The calculated age for tonalite sample D04 is 16.67 ±0.22 Ma (Fig. DR4-2), which is consistent with Ar-Ar dating results for volcanic rocks from Santo (see data repository DR3). Four U/Pb zircon analyses from dolerite sample BTM4 returned an age of 32.38 ±0.57 Ma (Fig. DR4-2), and several zircons of Miocene age were analysed from volcanic rock samples A01 and D01 (Table DR4-1). These zircon grains are not considered to have directly crystallized from their host rocks, but likely represent an inherited component derived from older volcanic sequences or plutons of Santo. Nevertheless, these data supplement the Ar-Ar and tonalite U/Pb ages in constraining the timing of igneous development of the Western Belt, Vanuatu.

Isotopic data derived from pre-Eocene zircon grains were discriminated initially based on age. Analytical spots with calculated $^{206}Pb/^{238}U$ ages below 1000 Ma were corrected for common Pb by utilizing the Age7Corr and AgeEr7Corr algorithms in Isoplot, with common Pb compositions modeled from Stacey and Kramers (1975). The resultant calculated ages were then subject to discordance analysis. Where grains were in excess of 1000 Ma the $^{207}Pb/^{206}Pb$ age was preferred and assessed for discordance between the $^{207}Pb/^{206}Pb$ and $^{206}Pb/^{238}U$ age systems. Grains less than 1000 Ma in age (common-Pb corrected) were reported according to the $^{206}Pb/^{238}U$ age and assessed for discordance between both $^{207}Pb/^{206}Pb$ and $^{206}Pb/^{238}U$, and $^{206}Pb/^{238}U$ and $^{207}Pb/^{235}U$ age systems. A conservative 15 %

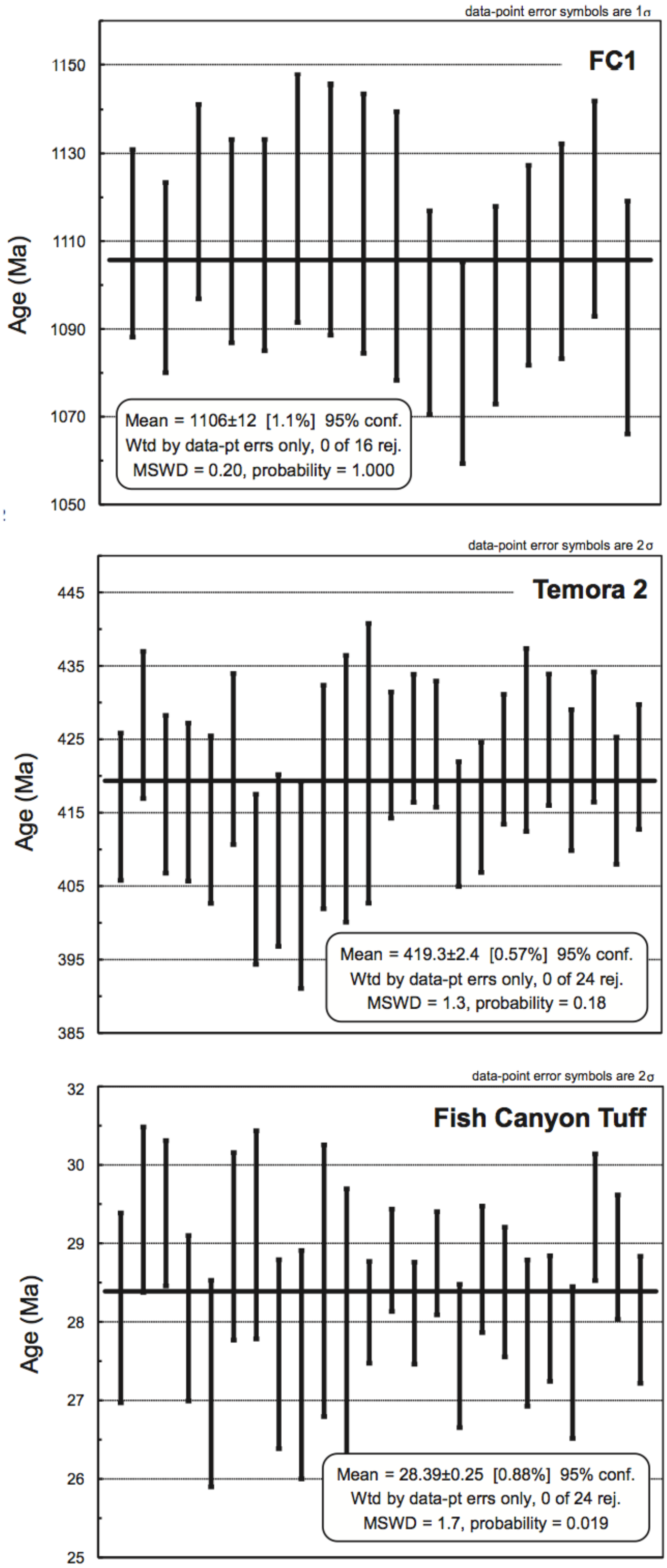

Figure DR4-1. Weighted mean $^{206}Pb/^{238}U$ ages for FC1, Temora 2 and Fish Canyon Tuff zircon standards.

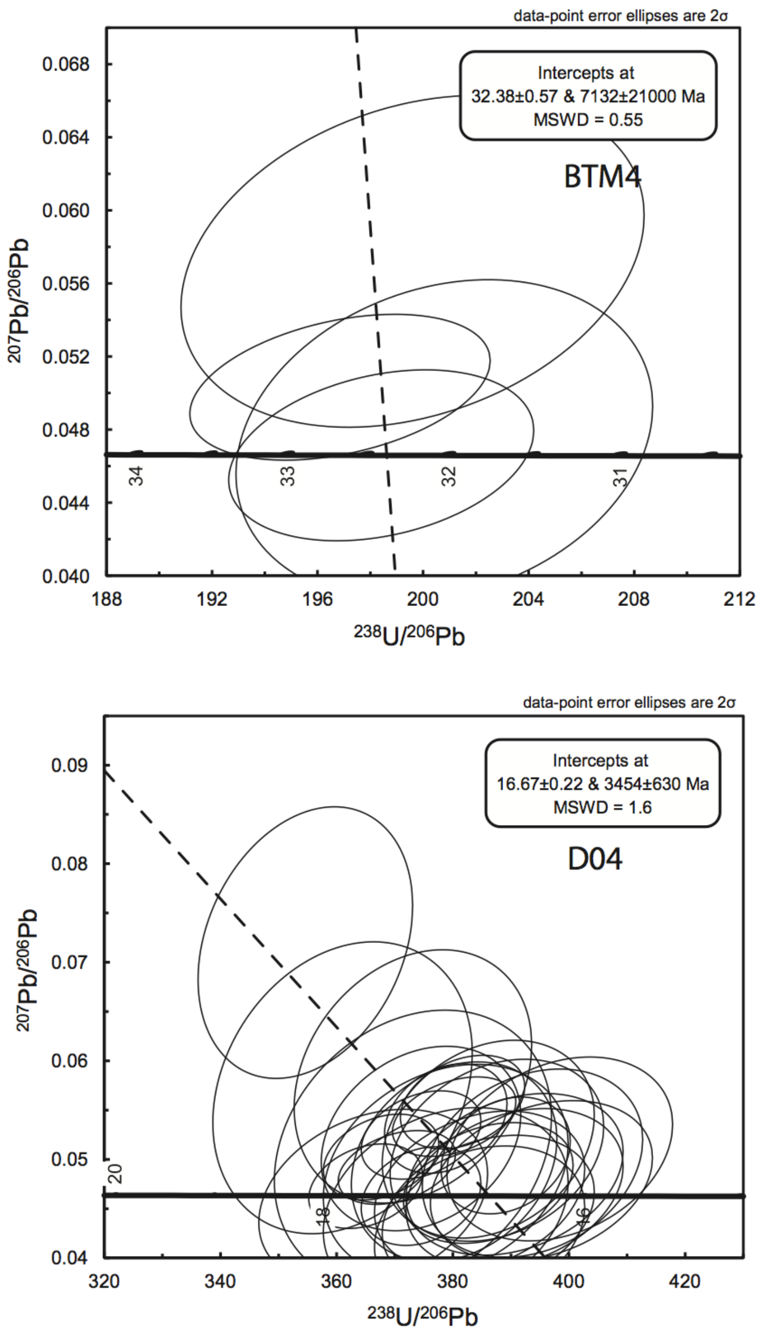

Figure DR4-2. U/Pb concordia plots for igneous zircons from samples BTM4 and D04

discordance threshold was used as the cut-off limit beyond which analyses were excluded from further data reduction. Comparison of results with higher discordance thresholds revealed no changes to the overall distribution of significant inherited age populations. The preferred inherited ages taken forward for analysis were a combination of $^{207}Pb/^{206}Pb$ and

$^{206}Pb/^{238}U$ ages and all errors were propagated and reported at 1σ level (Table DR4-1). These were plotted using the cumulative probability plot and histogram function of Isoplot.

Significant populations for Figure 1 in the manuscript were defined as those above background level, with background age populations removed for ease of presentation. Assignment of significant populations and background levels were based on proportions of semi-continuous age populations compared to the entire age spectrum. In this context a significant population is defined as a multiple of zircon ages that are within the 1σ level of age uncertainty from the next grain when sorted in a continuous age spectrum. For the results presented here for Vanuatu, the threshold above which a semi-continuous age population is regarded as significant is 4 zircon ages, or equivalent to approximately 2.5% of the entire population.

References:

Black, L. P., Kamo, S. L., Allen, C. M., Davis, D. W., Aleinkoff, J. N., Valley, J. W., Mudil, R., Campbell, I. H., Korsch, R. J., Williams, I. S., and Foudoulis, C., 2004, Improved $^{206}Pb/^{238}U$ microprobe geochronology by the monitoring of trace-element-related matrix effect; SHRIMP, ID-TIMS, ELA-ICP-MS and oxygen isotope documentation for a series of zircon standards. Chemical Geology, v. 205, p. 115–140.

Dobrzhinetskaya, L., Wirth, R., and Green, H., 2014, Diamonds in Earth's oldest zircons from Jack Hills conglomerate, Australia, are contamination. Earth and Planetary Science Letters, v. 387, p. 212-218.

Jackson, S. E., Pearson, N. J., Griffin, W. L., and Belousova, E. E., 2004, The application of laser ablation-inductively coupled plasma-mass spectrometry to in situ U-Pb zircon geochronology. Chemical Geology, v. 211, p. 47–69.

Ludwig, K. R., 2009, User's Manual for Isoplot 3.70: A Geochronological Toolkit for Microsoft Excel. Berkeley Geochronology Center Special Publication, v. 4.

Renne, P. R., Mundil, R., Balco, G., Min, K., and Ludwig, K. R., 2010, Joint determination of ^{40}K decay constants and ^{40}Ar*/^{40}K for the Fish Canyon sanidine standard, and improved accuracy for ^{40}Ar/^{39}Ar geochronology. Geochimica et Cosmochimica Acta, v. 74, p. 5349–5367.

Schmitz, M. D., and Bowring, S. A., 2001, U-Pb zircon and titanite systematics of the Fish Canyon Tuff: an assessment of high-precision U-Pb geochronology and its application to young volcanic rocks. Geochimica et Cosmochimica Acta, v. 65, p. 2571–2587.

Stacey, J. S., and Kramers, J. D., 1975, Approximation of terrestrial lead isotope evolution by a two-stage model. Earth and Planetary Science Letters, v. 26, p. 207–221.

Tera, F., and Wasserburg, G. J., 1972, U-Th-Pb systematics in three Apollo 14 basalts and the problem of initial Pb in lunar rocks. Earth and Planetary Science Letters, v. 14, p. 281–304.

Tucker, R. T., Roberts, E. M., Hu, Y., Kemp, A. I. S., and Salisbury, S. W., 2013, Detrital zircon age constraints for the Winton Formation, Queensland: Contextualizing Australia's Late Cretaceous dinosaur faunas. Gondwana Research, v. 24, p. 767-779.

Van Achterbergh, E., Ryan, C. G., Jackson, S. E., and Griffin, W. L., 2001, Appendix, in: Sylvester, P. J., ed., Laser Ablation-ICP-Mass Spectrometry in the Earth Sciences: Principle and Applications. Mineralogical Association of Canada (MAC) Short Course Series, v. 29, p. 239.

Table DR4-1. Isotope data and ages for magmatic zircons from Santo igneous roc

Sample	Analysis	Measured Isotope Ratios: $^{207}Pb/^{206}Pb$	2σ Error	$^{207}Pb/^{235}U$	2σ Error	$^{206}Pb/^{238}U$	2σ Error	Corrected $^{207}Pb/^{235}U$ Age	2σ Error
A01	13	0.05970	0.01472	0.02206	0.00532	0.00268	0.00014	17.0	0.9
	14	0.16295	0.02086	0.07327	0.00878	0.00326	0.00016	17.9	1.6
	15	0.05641	0.00870	0.02091	0.00316	0.00269	0.00010	17.1	0.7
BTM4	9	0.05032	0.00326	0.03524	0.00220	0.00508	0.00012	32.5	0.8
	10	0.04659	0.00382	0.03236	0.00256	0.00504	0.00012	32.4	0.8
	11	0.05721	0.00742	0.03947	0.00498	0.00501	0.00018	31.8	1.2
	12	0.04742	0.00718	0.03256	0.00484	0.00498	0.00016	32.0	1.1
D01	78	0.15768	0.01314	0.06653	0.00516	0.00306	0.00010	16.9	1.2
	92	0.31191	0.01942	0.20888	0.01142	0.00486	0.00016	20.7	4.2
D04	1	0.04849	0.00670	0.01714	0.00232	0.00256	0.00010	16.4	0.7
	2	0.05107	0.01150	0.01889	0.00416	0.00268	0.00014	17.2	0.9
	3	0.04680	0.00662	0.01680	0.00232	0.00260	0.00010	16.7	0.7
	4	0.05038	0.00722	0.01679	0.00236	0.00242	0.00010	15.5	0.7
	5	0.04461	0.00640	0.01594	0.00224	0.00259	0.00010	16.7	0.7
	6	0.04705	0.00662	0.01661	0.00228	0.00256	0.00010	16.5	0.7
	7	0.04313	0.00672	0.01547	0.00236	0.00260	0.00010	16.8	0.7
	8	0.07442	0.01018	0.02557	0.00340	0.00249	0.00010	15.5	0.7
	9	0.05424	0.00778	0.01837	0.00258	0.00246	0.00010	15.7	0.7
	10	0.05842	0.01050	0.02156	0.00378	0.00268	0.00012	17.0	0.8
	11	0.04784	0.00664	0.01665	0.00226	0.00253	0.00010	16.3	0.7
	12	0.05212	0.00764	0.01920	0.00274	0.00267	0.00010	17.1	0.7
	13	0.04605	0.00738	0.01733	0.00272	0.00273	0.00012	17.6	0.8
	14	0.05541	0.00746	0.01865	0.00246	0.00244	0.00010	15.5	0.7
	15	0.04976	0.00828	0.01804	0.00294	0.00263	0.00010	16.9	0.7
	16	0.05647	0.00792	0.01870	0.00256	0.00240	0.00010	15.3	0.7
	17	0.05726	0.01210	0.02187	0.00452	0.00277	0.00014	17.6	0.9
	18	0.05093	0.00754	0.01808	0.00262	0.00258	0.00010	16.5	0.7
	19	0.05338	0.00800	0.01835	0.00268	0.00249	0.00010	15.9	0.7
	20	0.05205	0.00820	0.01860	0.00286	0.00259	0.00010	16.6	0.7
	21	0.04885	0.00882	0.01781	0.00314	0.00264	0.00012	16.9	0.8
	22	0.04962	0.00780	0.01739	0.00268	0.00254	0.00010	16.3	0.7
	23	0.04516	0.00824	0.01643	0.00294	0.00264	0.00012	17.0	0.8
	24	0.05106	0.00762	0.01769	0.00258	0.00251	0.00010	16.1	0.7
	25	0.04718	0.00736	0.01600	0.00244	0.00246	0.00010	15.8	0.7
	26	0.07199	0.01126	0.02801	0.00428	0.00282	0.00012	17.6	0.8
	27	0.05040	0.00484	0.01788	0.00168	0.00257	0.00006	16.5	0.4
	28	0.04761	0.00500	0.01698	0.00174	0.00259	0.00008	16.6	0.5
	29	0.04628	0.00410	0.01706	0.00148	0.00267	0.00006	17.2	0.4
	30	0.05581	0.00388	0.02020	0.00136	0.00262	0.00006	16.7	0.4
	31	0.05248	0.00366	0.01935	0.00130	0.00267	0.00006	17.1	0.4
	32	0.05415	0.00454	0.01971	0.00160	0.00264	0.00006	16.8	0.4
	33	0.05023	0.00356	0.01886	0.00130	0.00272	0.00006	17.4	0.4
	34	0.04919	0.00306	0.01830	0.00110	0.00270	0.00006	17.3	0.4
	35	0.04728	0.00350	0.01783	0.00128	0.00274	0.00006	17.6	0.4
	36	0.05434	0.00330	0.01973	0.00116	0.00263	0.00006	16.8	0.4

Table DR4-2. Isotope data and ages for pre-Eocene inherited zircons from Santo volcanic rocks.

		Measured Isotope Ratios						Calculated Ages						Discordance		Preferred Age*	
Sample	Analysis	$^{207}Pb/^{206}Pb$	1σ Error	$^{207}Pb/^{235}U$	1σ Error	$^{206}Pb/^{238}U$	1σ Error	$^{207}Pb/^{206}Pb$ Age	1σ Error	$^{206}Pb/^{238}U$ Age	1σ Error	$^{207}Pb/^{235}U$ Age	1σ Error	Pb-Pb/U-Pb	U-Pb/U-Pb	Age (Ma)	1σ Error
A01	1	0.16759	0.00214	1.38685	0.01811	0.06003	0.00066	2534	11	323	5	883	8	87.3	63.4	323	5
	2	0.09884	0.00125	3.71544	0.04825	0.27268	0.00296	1602	12	1550	16	1575	10	3.3		**1602**	**12**
	3	0.09975	0.00128	4.05091	0.05302	0.29459	0.00319	1619	12	1669	18	1645	11	-3.1		**1619**	**12**
	4	0.11680	0.00147	4.96035	0.06396	0.30806	0.00332	1908	11	1710	18	1813	11	10.4		**1908**	**11**
	5	0.11978	0.00153	4.58617	0.05970	0.27772	0.00299	1953	11	1540	16	1747	11	21.1		1953	11
	6	0.09192	0.00125	2.45669	0.03372	0.19384	0.00210	1466	13	1124	12	1259	10	23.3		1466	13
	7	0.05641	0.00167	0.32543	0.00947	0.04184	0.00052	468	32	263	3	286	7	43.9	8.2	**263**	**3**
	8	0.13047	0.00171	2.69026	0.03559	0.14954	0.00160	2104	11	833	10	1326	10	60.4	37.2	833	10
	9	0.12824	0.00170	4.62102	0.06159	0.26132	0.00280	2074	12	1438	16	1753	11	30.7		2074	12
	10	0.05255	0.00107	0.29030	0.00585	0.04006	0.00045	309	23	253	3	259	5	18.3	2.3	**253**	**3**
	11	0.05203	0.00109	0.30402	0.00622	0.04237	0.00047	287	23	267	3	270	5	6.8	0.8	**267**	**3**
	12	0.06584	0.00116	1.22835	0.02122	0.13527	0.00147	801	18	818	9	814	10	-2.1	-0.6	**818**	**9**
	16	0.06890	0.00116	1.35582	0.02212	0.14270	0.00152	896	17	859	9	870	10	4.1	1.3	**859**	**9**
BTM4	1	0.11365	0.00165	4.14584	0.05840	0.26452	0.00276	1859	13	1480	15	1663	12	20.4		1859	13
	2	0.11473	0.00165	5.25968	0.07306	0.33243	0.00344	1876	13	1847	19	1862	12	1.5		**1876**	**13**
	3	0.05668	0.00470	1.04587	0.08464	0.13381	0.00301	478	87	819	18	727	42	-71.1	-12.6	**819**	**18**
	4	0.11572	0.00177	5.28954	0.07780	0.33147	0.00347	1891	14	1839	19	1867	13	2.7		**1891**	**14**
	5	0.13609	0.00294	0.93997	0.01910	0.05010	0.00057	2178	19	283	4	673	10	87.0	58.0	283	4
	6	0.11441	0.00180	5.53500	0.08149	0.35094	0.00356	1871	14	1949	20	1906	13	-4.2		**1871**	**14**
	7	0.09783	0.00163	3.72564	0.05815	0.27626	0.00283	1583	15	1572	16	1577	13	0.7		**1583**	**15**
	8	0.09157	0.00156	2.44505	0.03905	0.19371	0.00199	1458	16	1124	11	1256	12	23.0		1458	16
D01	1	0.18703	0.00336	10.85117	0.18023	0.42104	0.00444	2716	15	2151	26	2511	15	20.8		2716	15
	2	0.18704	0.00322	13.13566	0.20769	0.50967	0.00520	2716	14	2633	32	2689	15	3.1		**2716**	**14**
	3	0.08451	0.00302	0.84447	0.02991	0.07247	0.00090	1304	34	436	6	622	16	66.6	29.9	436	6
	4	0.05695	0.00207	0.58861	0.02119	0.07496	0.00093	489	39	466	6	470	14	4.7	0.9	**466**	**6**
	5	0.15323	0.00541	4.55816	0.15922	0.21574	0.00265	2382	29	1158	17	1742	29	51.4		2382	29
	6	0.17694	0.00628	5.55405	0.19496	0.22767	0.00281	2624	29	1184	19	1909	30	54.9		2624	29
	7	0.06612	0.00240	1.19551	0.04286	0.13114	0.00163	810	37	794	10	799	20	2.0	0.6	**794**	**10**
	8	0.04879	0.00207	0.24939	0.01044	0.03707	0.00049	138	48	235	3	226	8	-70.7	-4.0	**235**	**3**
	9	0.11721	0.00422	5.79029	0.20559	0.35833	0.00444	1914	32	1983	26	1945	31	-3.6		**1914**	**32**
	10	0.11431	0.00413	5.34832	0.19038	0.33938	0.00420	1869	32	1886	25	1877	30	-0.9		**1869**	**32**
	11	0.17943	0.00653	7.40295	0.26489	0.29927	0.00372	2648	30	1540	24	2161	32	41.8		2648	30
	12	0.18455	0.00676	10.68328	0.38443	0.41991	0.00526	2694	30	2152	33	2496	33	20.1		2694	30
	13	0.18667	0.00747	13.83131	0.53441	0.53755	0.00707	2713	32	2799	51	2738	37	-3.2		**2713**	**32**
	14	0.18425	0.00747	11.94263	0.46708	0.47024	0.00630	2692	33	2422	41	2600	37	10.0		**2692**	**33**
	15	0.18371	0.00738	12.36499	0.47894	0.48830	0.00636	2687	32	2522	42	2633	36	6.1		**2687**	**32**
	16	0.18547	0.00749	11.10612	0.43178	0.43445	0.00566	2702	33	2225	36	2532	36	17.7		2702	33
	17	0.05428	0.00234	0.43872	0.01823	0.05864	0.00078	383	47	367	5	369	13	4.0	0.6	**367**	**5**
	18	0.11977	0.00488	5.89282	0.23073	0.35697	0.00464	1953	36	1970	28	1960	34	-0.9		**1953**	**36**
	19	0.18352	0.00753	7.84478	0.30897	0.31012	0.00406	2685	33	1586	27	2213	35	40.9		2685	33
	20	0.17838	0.00734	11.09199	0.43718	0.45112	0.00588	2638	33	2333	38	2531	37	11.6		**2638**	**33**
	21	0.06544	0.00284	1.05174	0.04380	0.11660	0.00157	789	44	709	10	730	22	10.1	2.8	**709**	**10**
	22	0.06387	0.00273	1.05256	0.04312	0.11957	0.00159	737	44	728	10	730	21	1.3	0.3	**728**	**10**
	23	0.10743	0.00455	0.75717	0.03065	0.05114	0.00068	1756	38	300	4	572	18	82.9	47.6	300	4
	24	0.09945	0.00119	1.70472	0.02033	0.12433	0.00128	1614	11	724	8	1010	8	55.1	28.3	724	8
	25	0.06057	0.00074	0.77815	0.00948	0.09319	0.00096	624	13	573	6	584	5	8.1	1.9	**573**	**6**
	26	0.06743	0.00078	0.68760	0.00796	0.07396	0.00076	851	12	454	5	531	5	46.7	14.6	**454**	**5**
	27	0.07266	0.00080	1.58317	0.01753	0.15805	0.00161	1004	11	944	9	964	7	6.0	2.1	**944**	**9**
	28	0.09832	0.00107	3.82709	0.04189	0.28235	0.00288	1593	10	1604	16	1599	9	-0.7		**1593**	**10**
	29	0.06242	0.00070	0.90137	0.01014	0.10474	0.00107	689	12	641	6	653	5	6.9	1.7	**641**	**6**
	30	0.06456	0.00112	0.77488	0.01318	0.08706	0.00094	760	18	534	6	583	8	29.7	8.3	**534**	**6**
	31	0.06169	0.00087	0.91268	0.01271	0.10732	0.00112	663	15	657	7	659	7	0.9	0.2	**657**	**7**
	32	0.07783	0.00085	1.84226	0.02030	0.17169	0.00175	1143	11	1016	10	1061	7	11.1		**1143**	**11**
	33	0.07432	0.00082	1.57768	0.01751	0.15398	0.00157	1050	11	918	9	962	7	12.5	4.5	**918**	**9**
	34	0.10794	0.00117	4.53698	0.04925	0.30489	0.00309	1765	10	1710	17	1738	9	3.1		**1765**	**10**
	35	0.06909	0.00128	0.46735	0.00846	0.04907	0.00053	901	19	302	3	389	6	66.4	22.3	302	3
	36	0.05814	0.00072	0.68724	0.00849	0.08574	0.00088	535	14	530	5	531	5	0.8	0.2	**530**	**5**
	37	0.12275	0.00133	5.63708	0.06099	0.33311	0.00337	1997	10	1834	18	1922	9	8.2		**1997**	**10**
	38	0.07243	0.00083	1.36250	0.01565	0.13644	0.00139	998	12	819	8	873	7	18.0	6.2	**819**	**8**
	39	0.07378	0.00087	1.35355	0.01581	0.13307	0.00136	1036	12	798	8	869	7	22.9	8.2	**798**	**8**
	40	0.05815	0.00074	0.69120	0.00870	0.08622	0.00088	535	14	533	5	534	5	0.3	0.1	**533**	**5**
	41	0.10613	0.00116	3.25279	0.03542	0.22230	0.00225	1734	10	1261	13	1470	8	27.3		1734	10
	42	0.22285	0.00244	16.16045	0.17636	0.52600	0.00533	3001	9	2602	32	2886	10	13.3		**3001**	**9**
	43	0.08310	0.00096	1.63288	0.01882	0.14254	0.00145	1272	11	843	8	983	7	33.7	14.2	**843**	**8**
	44	0.06616	0.00132	0.21434	0.00418	0.02350	0.00026	812	21	147	2	197	4	81.9	25.7	147	2
	45	0.05661	0.00115	0.22235	0.00444	0.02849	0.00031	476	22	180	2	204	4	62.3	11.9	**180**	**2**

	46	0.09374	0.00110	3.26842	0.03816	0.25290	0.00257	1503	11	1449	14	1474	9	3.6		**1503**	**11**
	47	0.07109	0.00087	0.99919	0.01204	0.10195	0.00104	960	12	618	6	703	6	35.6	12.1	**618**	**6**
	48	0.07156	0.00134	0.24431	0.00448	0.02477	0.00027	973	19	153	2	222	4	84.2	30.9	153	2
	49	0.10100	0.00114	4.19269	0.04708	0.30110	0.00304	1643	10	1702	17	1673	9	-3.6		**1643**	**10**
	50	0.06202	0.00093	0.60509	0.00888	0.07077	0.00073	675	16	437	4	481	6	35.2	9.0	**437**	**4**
	51	0.18347	0.00209	9.60093	0.10825	0.37958	0.00384	2685	9	1943	22	2397	10	27.6		2685	9
	52	0.12151	0.00138	4.95302	0.05582	0.29567	0.00298	1979	10	1635	16	1811	10	17.4		1979	10
	53	0.05801	0.00079	0.67331	0.00909	0.08420	0.00086	530	15	521	5	523	6	1.6	0.3	**521**	**5**
	54	0.10404	0.00127	3.83518	0.04617	0.26740	0.00272	1697	11	1512	15	1600	10	10.9		**1697**	**11**
	55	0.12332	0.00146	2.87795	0.03349	0.16928	0.00171	2005	10	949	10	1376	9	52.6	31.0	949	10
	56	0.07434	0.00093	1.64809	0.02033	0.16082	0.00163	1051	13	958	9	989	8	8.8	3.1	**958**	**9**
	57	0.08341	0.00102	2.40207	0.02881	0.20890	0.00212	1279	12	1220	12	1243	9	4.6		**1279**	**12**
	58	0.08035	0.00106	2.06190	0.02664	0.18614	0.00190	1206	13	1095	11	1136	9	9.2		**1206**	**13**
	59	0.09811	0.00116	3.59875	0.04192	0.26607	0.00268	1589	11	1515	15	1549	9	4.6		**1589**	**11**
	60	0.06533	0.00138	1.00737	0.02083	0.11185	0.00124	785	22	681	7	708	11	13.3	3.7	**681**	**7**
	61	0.05985	0.00074	0.73317	0.00896	0.08886	0.00090	598	13	548	5	558	5	8.4	1.9	**548**	**5**
	62	0.07494	0.00122	1.72894	0.02747	0.16736	0.00177	1067	16	995	10	1019	10	6.8	2.4	**995**	**10**
	63	0.05264	0.00069	0.22366	0.00289	0.03082	0.00031	313	15	195	2	205	2	37.7	4.9	**195**	**2**
	64	0.07007	0.00091	1.26915	0.01612	0.13138	0.00133	931	13	792	8	832	7	14.9	4.9	**792**	**8**
	65	0.06067	0.00091	0.79609	0.01169	0.09519	0.00098	628	16	585	6	595	7	6.7	1.6	**585**	**6**
	66	0.08174	0.00116	0.95189	0.01314	0.08447	0.00087	1239	14	508	5	679	7	59.0	25.2	508	5
	67	0.18517	0.00201	10.20253	0.10100	0.39965	0.00365	2700	9	2041	21	2453	9	24.4		2700	9
	68	0.18559	0.00202	9.98348	0.09909	0.39019	0.00357	2704	9	1992	21	2433	9	26.3		2704	9
	69	0.17187	0.00184	11.07250	0.10807	0.46729	0.00425	2576	9	2442	24	2529	9	5.2		**2576**	**9**
	70	0.11533	0.00126	5.51489	0.05491	0.34686	0.00316	1885	10	1924	18	1903	9	-2.1		**1885**	**10**
	71	0.11341	0.00123	5.00215	0.04933	0.31993	0.00291	1855	10	1781	16	1820	8	4.0		**1855**	**10**
	72	0.13072	0.00141	5.31691	0.05237	0.29503	0.00268	2108	9	1612	15	1872	8	23.5		2108	9
	73	0.17804	0.00194	4.41271	0.04389	0.17977	0.00164	2635	9	938	11	1715	8	64.4	45.3	938	11
	74	0.18449	0.00203	11.07405	0.11094	0.43539	0.00398	2694	9	2232	23	2529	9	17.1		2694	9
	75	0.12383	0.00135	6.37550	0.06315	0.37346	0.00339	2012	10	2051	19	2029	9	-1.9		**2012**	**10**
	76	0.11718	0.00128	5.66262	0.05625	0.35051	0.00318	1914	10	1940	18	1926	9	-1.4		**1914**	**10**
	77	0.08366	0.00105	2.23706	0.02612	0.19397	0.00180	1284	12	1135	10	1193	8	11.6		**1284**	**12**
	79	0.11572	0.00131	5.36637	0.05564	0.33636	0.00307	1891	10	1866	17	1880	9	1.3		**1891**	**10**
	80	0.16587	0.00183	9.80056	0.09862	0.42859	0.00390	2516	9	2246	22	2416	9	10.7		**2516**	**9**
	81	0.18611	0.00206	7.96376	0.08033	0.31038	0.00283	2708	9	1582	18	2227	9	41.6		2708	9
	82	0.06565	0.00089	1.05896	0.01332	0.11701	0.00108	795	14	711	6	733	7	10.5	3.0	**711**	**6**
	83	0.11314	0.00129	5.13043	0.05332	0.32890	0.00300	1851	10	1831	17	1841	9	1.1		**1851**	**10**
	84	0.18776	0.00213	13.54386	0.13984	0.52321	0.00480	2723	9	2709	29	2718	10	0.5		**2723**	**9**
	85	0.18422	0.00205	13.50303	0.13636	0.53167	0.00484	2691	9	2772	30	2716	10	-3.0		**2691**	**9**
	86	0.11537	0.00127	5.12349	0.05133	0.32213	0.00291	1886	10	1789	16	1840	9	5.1		**1886**	**10**
	87	0.05773	0.00096	0.34131	0.00534	0.04289	0.00041	519	18	269	3	298	4	48.2	9.9	**269**	**3**
	88	0.16729	0.00188	7.22696	0.07367	0.31336	0.00284	2531	9	1635	17	2140	9	35.4		2531	9
	89	0.08008	0.00096	2.20695	0.02431	0.19991	0.00182	1199	12	1174	10	1183	8	2.1		**1199**	**12**
	90	0.13559	0.00151	6.95362	0.07008	0.37199	0.00336	2172	10	2016	19	2106	9	7.2		**2172**	**10**
	91	0.05424	0.00084	0.26817	0.00390	0.03586	0.00033	381	17	226	2	241	3	40.6	6.3	**226**	**2**
	93	0.18034	0.00192	11.97462	0.12521	0.48180	0.00477	2656	9	2497	27	2602	10	6.0		**2656**	**9**
	94	0.16251	0.00174	8.21163	0.08623	0.36663	0.00363	2482	9	1926	20	2255	10	22.4		2482	9
	95	0.18376	0.00203	11.74241	0.12675	0.46364	0.00463	2687	9	2388	26	2584	10	11.1		**2687**	**9**
	96	0.14564	0.00161	8.61897	0.09349	0.42938	0.00428	2295	9	2305	24	2299	10	-0.4		**2295**	**9**
	97	0.18462	0.00319	6.90503	0.11374	0.27137	0.00313	2695	14	1392	19	2099	15	48.3		2695	14
	98	0.18530	0.00205	12.51183	0.13501	0.48989	0.00488	2701	9	2526	28	2644	10	6.5		**2701**	**9**
	99	0.11954	0.00129	5.97993	0.06319	0.36294	0.00359	1949	10	2003	20	1973	9	-2.8		**1949**	**10**
	##	0.23080	0.00252	12.53292	0.13370	0.39397	0.00391	3058	9	1894	25	2645	10	38.0		3058	9
	##	0.16585	0.00183	10.91875	0.11741	0.47764	0.00474	2516	9	2517	27	2516	10	0.0		**2516**	**9**
	##	0.16703	0.00186	10.86264	0.11798	0.47183	0.00470	2528	9	2481	27	2511	10	1.9		**2528**	**9**
	##	0.20842	0.00223	15.66674	0.16337	0.54536	0.00537	2893	9	2765	33	2857	10	4.4		**2893**	**9**
D02	1	0.18292	0.01327	12.66660	0.89931	0.50216	0.01019	2680	58	2603	73	2655	67	2.9		**2680**	**58**
	2	0.18684	0.01361	12.09263	0.86170	0.46934	0.00956	2715	58	2409	65	2612	67	11.2		**2715**	**58**
	3	0.16109	0.01177	9.66764	0.69128	0.43521	0.00888	2467	59	2295	58	2404	66	7.0		**2467**	**59**
	4	0.18453	0.01355	12.97735	0.93215	0.51000	0.01050	2694	58	2643	75	2678	68	1.9		**2694**	**58**
	5	0.18308	0.01371	8.69014	0.63556	0.34424	0.00715	2681	59	1763	47	2306	67	34.2		2681	59
	6	0.05244	0.00407	0.34951	0.02651	0.04834	0.00102	305	84	304	7	304	20	0.1	0.0	**304**	**7**
	7	0.05634	0.00428	0.62889	0.04663	0.08095	0.00169	465	80	502	11	495	29	-8.0	-1.4	**502**	**11**
	8	0.20701	0.01562	15.52939	1.14416	0.54407	0.01131	2882	59	2763	88	2848	70	4.1		**2882**	**59**
	9	0.11636	0.00888	4.37699	0.32609	0.27282	0.00576	1901	66	1520	35	1708	62	20.1		1901	66
	10	0.07701	0.00587	1.49373	0.11109	0.14068	0.00294	1121	72	839	18	928	45	25.2	9.6	**839**	**18**
	11	0.11558	0.00881	5.55337	0.41333	0.34849	0.00729	1889	66	1933	44	1909	64	-2.3		**1889**	**66**
	12	0.14862	0.01137	6.28084	0.46887	0.30652	0.00643	2330	63	1641	40	2016	65	29.6		2330	63
	13	0.11405	0.00877	5.38467	0.40367	0.34243	0.00721	1865	66	1903	44	1882	64	-2.0		**1865**	**66**
	14	0.11349	0.00875	5.36473	0.40340	0.34284	0.00723	1856	67	1906	44	1879	64	-2.7		**1856**	**67**
	15	0.11629	0.00915	5.69086	0.43619	0.35495	0.00759	1900	68	1967	46	1930	66	-3.5		**1900**	**68**
	16	0.14343	0.01132	6.06811	0.46631	0.30688	0.00658	2269	65	1653	41	1986	67	27.2		2269	65
	17	0.10460	0.00830	3.85854	0.29823	0.26758	0.00577	1707	70	1512	35	1605	62	11.4		**1707**	**70**
	18	0.18040	0.01435	8.48108	0.65685	0.34102	0.00738	2657	63	1753	49	2284	70	34.0		2657	63
	19	0.19535	0.01558	8.86851	0.68847	0.32932	0.00712	2788	62	1663	49	2325	71	40.3		2788	62

20	0.08871	0.00713	0.53970	0.04221	0.04413	0.00096	1398	73	266	6	438	28	81.0	39.4	266	6
21	0.05226	0.00442	0.27464	0.02263	0.03812	0.00086	297	91	241	6	246	18	18.8	2.3	**241**	**6**
22	0.10276	0.00865	0.55207	0.04513	0.03897	0.00090	1675	74	231	6	446	30	86.2	48.3	231	6
23	0.21985	0.01777	7.80368	0.61333	0.25750	0.00562	2980	62	1260	42	2209	71	57.7		2980	62
24	0.18463	0.01499	11.06327	0.87356	0.43469	0.00955	2695	64	2228	65	2529	74	17.3		2695	64
25	0.08422	0.00712	0.99959	0.08210	0.08611	0.00197	1298	78	516	12	704	42	60.3	26.7	516	12
26	0.06781	0.00567	1.28274	0.10433	0.13724	0.00308	863	82	828	19	838	46	4.0	1.2	**828**	**19**
27	0.05544	0.00460	0.27613	0.02228	0.03613	0.00080	430	88	227	5	248	18	47.1	8.1	**227**	**5**
28	0.05575	0.00465	0.30612	0.02480	0.03984	0.00089	442	88	250	6	271	19	43.3	7.7	**250**	**6**
29	0.18710	0.01545	8.30593	0.66602	0.32207	0.00714	2717	65	1638	49	2265	73	39.7		2717	65
30	0.18305	0.01517	13.15152	1.05876	0.52125	0.01162	2681	65	2714	86	2691	76	-1.2		**2681**	**65**
31	0.07494	0.00254	0.15754	0.00519	0.01525	0.00021	1067	33	94	1	149	5	91.2	36.6	94	1
32	0.05493	0.00104	0.32202	0.00605	0.04252	0.00048	409	21	267	3	284	5	34.7	5.7	**267**	**3**
33	0.17976	0.00330	0.53609	0.00972	0.02163	0.00024	2651	15	115	2	436	6	95.7	73.6	115	2
34	0.05676	0.00109	0.39352	0.00752	0.05028	0.00056	482	21	315	3	337	5	34.7	6.6	**315**	**3**
35	0.21469	0.00384	1.72316	0.03058	0.05822	0.00065	2941	14	292	5	1017	11	90.1	71.3	292	5
36	0.14142	0.00251	0.89048	0.01570	0.04567	0.00051	2245	15	256	3	647	8	88.6	60.4	256	3
37	0.12569	0.00239	1.09428	0.02061	0.06315	0.00071	2039	17	360	5	751	10	82.3	52.0	360	5
38	0.53887	0.00992	6.76989	0.12371	0.09113	0.00103	4351	13	225	20	2082	16	94.8	89.2	225	20
39	0.18636	0.00348	0.95949	0.01781	0.03734	0.00042	2710	15	197	3	683	9	92.7	71.2	197	3
40	0.09799	0.00183	0.78539	0.01458	0.05814	0.00065	1586	17	344	4	589	8	78.3	41.5	344	4
41	0.06860	0.00147	0.25744	0.00546	0.02722	0.00031	887	22	169	2	233	4	80.9	27.3	169	2
42	0.11888	0.00221	4.61826	0.08567	0.28178	0.00317	1940	16	1564	18	1753	15	19.4		1940	16
43	0.06257	0.00137	0.29105	0.00632	0.03374	0.00039	694	23	211	2	259	5	69.6	18.8	211	2
44	0.34447	0.00641	17.61687	0.32638	0.37096	0.00417	3683	14	1502	40	2969	18	59.2		3683	14
45	0.10283	0.00206	0.64205	0.01276	0.04529	0.00052	1676	18	268	3	504	8	84.0	46.9	268	3
46	0.22653	0.00426	2.14414	0.04014	0.06865	0.00077	3028	15	337	7	1163	13	88.9	71.0	337	7
47	0.12742	0.00253	0.64482	0.01271	0.03671	0.00042	2063	17	210	3	505	8	89.8	58.4	210	3
48	0.05465	0.00129	0.32183	0.00749	0.04272	0.00050	398	26	269	3	283	6	32.5	5.2	**269**	**3**
49	0.12035	0.00233	5.19305	0.10009	0.31299	0.00355	1961	17	1730	20	1852	16	11.8		**1961**	**17**
50	0.06759	0.00138	0.50005	0.01013	0.05366	0.00061	856	21	331	4	412	7	61.3	19.6	331	4
51	0.20535	0.00403	1.24391	0.02425	0.04394	0.00050	2869	16	224	4	821	11	92.2	72.6	224	4
52	0.13586	0.00268	1.13322	0.02224	0.06050	0.00069	2175	17	340	5	769	11	84.3	55.7	340	5
53	0.07113	0.00143	0.44788	0.00893	0.04567	0.00052	961	20	281	3	376	6	70.8	25.2	281	3
54	0.11981	0.00246	0.52333	0.01065	0.03168	0.00037	1953	18	184	2	427	7	90.6	57.0	184	2
55	0.06027	0.00139	0.22411	0.00511	0.02697	0.00032	613	25	169	2	205	4	72.4	17.6	169	2
56	0.08973	0.00189	0.52602	0.01101	0.04252	0.00049	1420	20	256	3	429	7	82.0	40.4	256	3
57	0.09322	0.00213	2.26341	0.05116	0.17612	0.00210	1492	21	1023	12	1201	16	31.5		1492	21
58	0.10998	0.00224	2.54567	0.05159	0.16789	0.00193	1799	18	957	11	1285	15	46.8	25.5	957	11
59	0.08853	0.00212	0.53670	0.01271	0.04397	0.00053	1394	23	265	3	436	8	81.0	39.3	265	3
60	0.16267	0.00346	0.89958	0.01894	0.04011	0.00047	2484	18	219	3	652	10	91.2	66.5	219	3
61	0.20781	0.00436	1.21240	0.02526	0.04232	0.00049	2889	17	215	4	806	12	92.5	73.3	215	4
62	0.08612	0.00189	0.47938	0.01042	0.04038	0.00047	1341	21	244	3	398	7	81.8	38.6	244	3
63	0.15729	0.00338	0.45149	0.00961	0.02082	0.00024	2427	18	114	2	378	7	95.3	69.7	114	2
64	0.19561	0.00422	0.63551	0.01357	0.02357	0.00028	2790	17	122	2	500	8	95.6	75.5	122	2
65	0.29149	0.00624	2.84904	0.06034	0.07090	0.00084	3426	16	312	9	1369	16	90.9	77.2	312	9
66	0.07492	0.00168	1.31957	0.02930	0.12775	0.00150	1067	22	766	9	854	13	28.2	10.3	**766**	**9**
67	0.05402	0.00127	0.33748	0.00789	0.04531	0.00054	372	26	285	3	295	6	23.4	3.5	**285**	**3**
68	0.13122	0.00312	0.83893	0.01970	0.04637	0.00057	2114	21	264	4	619	11	87.5	57.4	264	4
69	0.05481	0.00139	0.11660	0.00292	0.01543	0.00019	404	27	98	1	112	3	75.8	12.6	**98**	**1**
70	0.12458	0.00270	1.07551	0.02318	0.06262	0.00073	2023	19	358	5	741	11	82.3	51.8	358	5
71	0.07664	0.00183	0.42774	0.01012	0.04048	0.00048	1112	23	248	3	362	7	77.7	31.5	248	3
72	0.05780	0.00105	0.32720	0.00564	0.04106	0.00040	522	20	257	3	287	4	50.7	10.5	**257**	**3**
73	0.05425	0.00091	0.32347	0.00511	0.04325	0.00041	381	19	272	3	285	4	28.6	4.4	**272**	**3**
74	0.05569	0.00135	0.32691	0.00763	0.04258	0.00044	440	26	267	3	287	6	39.2	6.9	**267**	**3**
75	0.17669	0.00197	9.43469	0.09541	0.38731	0.00349	2622	9	1999	20	2381	9	23.8	16.0	2622	9
76	0.23290	0.00264	15.86970	0.16310	0.49425	0.00449	3072	9	2403	28	2869	10	21.8	16.2	3072	9
77	0.05819	0.00096	0.36105	0.00564	0.04500	0.00043	536	18	282	3	313	4	47.5	10.0	**282**	**3**
78	0.17795	0.00207	11.39677	0.12041	0.46455	0.00423	2634	10	2409	24	2556	10	8.5		**2634**	**10**
79	0.14914	0.00169	8.04079	0.08237	0.39107	0.00352	2336	10	2086	20	2236	9	10.7		**2336**	**10**
80	0.15842	0.00183	8.90169	0.09319	0.40757	0.00369	2439	10	2153	20	2328	10	11.7		**2439**	**10**
81	0.05528	0.00086	0.31327	0.00459	0.04111	0.00038	423	17	258	2	277	4	38.9	6.6	**258**	**2**
82	0.09278	0.00124	0.47383	0.00583	0.03704	0.00034	1483	13	222	2	394	4	85.0	43.6	222	2
83	0.05758	0.00079	0.49786	0.00636	0.06272	0.00057	513	15	391	4	410	4	23.9	4.8	**391**	**4**
84	0.06678	0.00113	1.16290	0.01854	0.12631	0.00121	831	17	765	7	783	9	7.9	2.3	**765**	**7**
85	0.05980	0.00089	0.60217	0.00838	0.07304	0.00068	597	16	452	4	479	5	24.2	5.5	**452**	**4**
86	0.06385	0.00095	0.63690	0.00885	0.07236	0.00067	737	16	446	4	500	5	39.4	10.9	**446**	**4**
87	0.16569	0.00194	10.76386	0.11389	0.47121	0.00426	2515	10	2481	25	2503	10	1.3		**2515**	**10**
88	0.05764	0.00078	0.53837	0.00676	0.06774	0.00062	516	15	421	4	437	4	18.4	3.7	**421**	**4**
89	0.06534	0.00115	1.05176	0.01743	0.11675	0.00112	785	18	710	7	730	9	9.6	2.7	**710**	**7**
90	0.06713	0.00119	1.11673	0.01862	0.12066	0.00116	842	18	731	7	761	9	13.1	3.9	**731**	**7**
91	0.06782	0.00083	1.21587	0.01358	0.13004	0.00117	863	13	786	7	808	6	8.9	2.7	**786**	**7**
92	0.12270	0.00146	5.09648	0.05474	0.30127	0.00271	1996	10	1662	15	1836	9	16.7		1996	10
93	0.17881	0.00212	10.79619	0.11584	0.43795	0.00394	2642	10	2261	22	2506	10	14.4		**2642**	**10**
94	0.12273	0.00149	6.42500	0.07061	0.37972	0.00343	1996	11	2088	19	2036	10	-4.6		**1996**	**11**

	95	0.18479	0.00222	9.96124	0.10826	0.39100	0.00353	2696	10	1998	21	2431	10	25.9		2696	10
	96	0.16720	0.00206	10.43468	0.11677	0.45267	0.00412	2530	10	2373	24	2474	10	6.2		**2530**	**10**
	97	0.20227	0.00242	14.36205	0.15498	0.51504	0.00463	2845	10	2612	28	2774	10	8.2		**2845**	**10**
	98	0.08554	0.00123	2.48888	0.03302	0.21105	0.00195	1328	14	1229	11	1269	10	7.4		**1328**	**14**
	99	0.17387	0.00212	10.48856	0.11515	0.43755	0.00393	2595	10	2273	22	2479	10	12.4		**2595**	**10**
	##	0.11424	0.00148	4.99628	0.05869	0.31722	0.00288	1868	12	1765	16	1819	10	5.5		**1868**	**12**
	##	0.11613	0.00148	5.15659	0.05967	0.32207	0.00292	1898	11	1787	16	1846	10	5.8		**1898**	**11**
	##	0.16020	0.00203	10.06544	0.11551	0.45573	0.00414	2458	11	2411	24	2441	11	1.9		**2458**	**11**
	##	0.07053	0.00082	1.33830	0.01512	0.13766	0.00136	944	12	828	8	863	7	12.3	4.0	**828**	**8**
	##	0.07467	0.00087	1.70184	0.01932	0.16534	0.00163	1060	12	983	9	1009	7	7.2	2.6	**983**	**9**
	##	0.18571	0.00208	10.04709	0.10929	0.39247	0.00389	2705	9	2003	22	2439	10	25.9		2705	9
	##	0.18456	0.00205	9.34339	0.10082	0.36726	0.00363	2694	9	1875	21	2372	10	30.4		2694	9
	##	0.13590	0.00151	7.94813	0.08590	0.42426	0.00418	2176	10	2302	24	2225	10	-5.8		**2176**	**10**
	##	0.11427	0.00127	5.57220	0.06024	0.35373	0.00348	1868	10	1964	19	1912	9	-5.1		**1868**	**10**
	##	0.12758	0.00145	6.97736	0.07703	0.39675	0.00392	2065	10	2170	22	2109	10	-5.1		**2065**	**10**
	##	0.07178	0.00081	1.52015	0.01673	0.15363	0.00151	980	11	919	9	939	7	6.2	2.1	**919**	**9**
	##	0.05963	0.00092	0.68777	0.01031	0.08367	0.00085	590	17	517	5	532	6	12.4	2.8	**517**	**5**
	##	0.11425	0.00133	5.50537	0.06197	0.34956	0.00345	1868	10	1942	19	1901	10	-3.9		**1868**	**10**
	##	0.18616	0.00210	9.33672	0.10153	0.36380	0.00357	2709	9	1854	21	2372	10	31.5		2709	9
	##	0.17426	0.00195	9.78063	0.10567	0.40712	0.00398	2599	9	2108	22	2414	10	18.9		2599	9
	##	0.05445	0.00082	0.29379	0.00428	0.03913	0.00039	390	17	246	2	262	3	36.8	5.8	**246**	**2**
	##	0.05687	0.00081	0.56167	0.00773	0.07164	0.00071	486	16	445	4	453	5	8.3	1.6	**445**	**4**
	##	0.06644	0.00097	1.14377	0.01622	0.12486	0.00125	820	15	757	7	774	8	7.8	2.3	**757**	**7**
	##	0.11176	0.00125	4.59162	0.04968	0.29800	0.00290	1828	10	1665	16	1748	9	8.9		**1828**	**10**
	##	0.12997	0.00154	6.76547	0.07730	0.37757	0.00372	2098	10	2059	21	2081	10	1.8		**2098**	**10**
	##	0.05501	0.00092	0.37339	0.00607	0.04923	0.00050	413	18	309	3	322	4	25.2	4.1	**309**	**3**
	##	0.05767	0.00088	0.55785	0.00824	0.07016	0.00070	517	17	436	4	450	5	15.6	3.1	**436**	**4**
	##	0.10682	0.00161	4.25206	0.06160	0.28872	0.00298	1746	14	1623	17	1684	12	7.0		**1746**	**14**
	##	0.17145	0.00212	11.46240	0.13625	0.48491	0.00483	2572	10	2541	28	2562	11	1.2		**2572**	**10**
	##	0.11508	0.00132	5.44634	0.05994	0.34329	0.00333	1881	10	1905	18	1892	9	-1.3		**1881**	**10**
	##	0.06555	0.00078	1.17827	0.01348	0.13038	0.00127	792	12	790	7	791	6	0.3	0.1	**790**	**7**
	##	0.05548	0.00079	0.39773	0.00543	0.05200	0.00051	431	15	326	3	340	4	24.4	4.2	**326**	**3**
	##	0.11495	0.00137	5.45044	0.06203	0.34391	0.00335	1879	11	1909	19	1893	10	-1.6		**1879**	**11**
	##	0.12244	0.00145	5.97248	0.06789	0.35382	0.00345	1992	10	1947	19	1972	10	2.3		**1992**	**10**
	##	0.15103	0.00176	9.20534	0.10255	0.44209	0.00429	2358	10	2361	24	2359	10	-0.1		**2358**	**10**
	##	0.11211	0.00163	5.03624	0.07018	0.32583	0.00332	1834	13	1816	18	1825	12	1.0		**1834**	**13**
D03	1	0.08652	0.00315	0.61844	0.02212	0.05185	0.00071	1350	34	312	4	489	14	76.9	36.1	312	4
	2	0.12109	0.00443	5.50038	0.19745	0.32951	0.00450	1972	32	1818	26	1901	31	7.8		**1972**	**32**
	3	0.26811	0.00983	9.91888	0.35702	0.26836	0.00368	3295	28	1225	30	2427	33	62.8		3295	28
	4	0.08861	0.00360	0.81357	0.03233	0.06660	0.00097	1396	38	399	6	605	18	71.4	34.0	399	6
	5	0.06029	0.00226	0.38814	0.01426	0.04670	0.00064	614	39	291	4	333	10	52.6	12.5	**291**	**4**
	6	0.20879	0.00782	13.06355	0.48091	0.45387	0.00627	2896	30	2261	40	2684	35	21.9		2896	30
	7	0.08599	0.00337	0.38310	0.01473	0.03232	0.00046	1338	37	196	3	329	11	85.4	40.5	196	3
	8	0.09733	0.00383	0.59822	0.02310	0.04458	0.00064	1574	36	265	4	476	15	83.1	44.3	265	4
	9	0.07628	0.00298	0.33949	0.01300	0.03228	0.00046	1103	38	198	3	297	10	82.0	33.2	198	3
	10	0.05443	0.00239	0.35303	0.01520	0.04705	0.00070	389	48	296	4	307	11	24.0	3.7	**296**	**4**
	11	0.13757	0.00560	0.83506	0.03321	0.04403	0.00065	2197	35	248	4	616	18	88.7	59.7	248	4
	12	0.13051	0.00518	0.56691	0.02207	0.03151	0.00046	2105	34	180	3	456	14	91.4	60.5	180	3
	13	0.05584	0.00220	0.54437	0.02105	0.07072	0.00100	446	43	440	6	441	14	1.1	0.2	**440**	**6**
	14	0.06801	0.00268	0.35357	0.01369	0.03771	0.00053	869	40	234	3	307	10	73.1	24.0	234	3
	15	0.44116	0.01698	2.60275	0.09847	0.04280	0.00060	4056	28	139	9	1301	28	96.6	89.3	139	9
	16	0.08594	0.00341	1.16928	0.04568	0.09869	0.00141	1337	37	588	9	786	21	56.0	25.2	588	9
	17	0.11365	0.00446	5.19260	0.20032	0.33144	0.00470	1859	35	1844	27	1851	33	0.8		**1859**	**35**
	18	0.17781	0.00699	12.20978	0.47241	0.49813	0.00708	2633	32	2597	46	2621	36	1.4		**2633**	**32**
	19	0.07593	0.00300	1.90498	0.07401	0.18199	0.00259	1093	39	1077	15	1083	26	1.5		**1093**	**39**
	20	0.33684	0.01330	7.41819	0.28824	0.15975	0.00227	3649	30	653	25	2163	35	82.1	69.8	653	25
	21	0.11919	0.00473	5.47840	0.21409	0.33341	0.00476	1944	35	1843	28	1897	34	5.2		**1944**	**35**
	22	0.07876	0.00314	3.21286	0.12605	0.29591	0.00423	1166	38	1715	25	1460	30	-47.1		1166	38
	23	0.21588	0.00862	14.64761	0.57557	0.49220	0.00707	2950	32	2444	47	2793	37	17.1		2950	32
	24	0.11313	0.00457	0.98974	0.03936	0.06346	0.00092	1850	36	368	6	699	20	80.1	47.3	368	6
	25	0.53342	0.02138	12.07173	0.47637	0.16417	0.00236	4336	29	423	41	2610	37	90.2	83.8	423	41
	26	0.14281	0.00574	6.78851	0.26864	0.34483	0.00495	2262	34	1853	29	2084	35	18.0		2262	34
	27	0.12299	0.00497	1.06326	0.04235	0.06271	0.00090	2000	35	359	6	735	21	82.1	51.2	359	6
	28	0.06996	0.00292	1.02757	0.04218	0.10654	0.00156	927	42	646	9	718	21	30.3	10.0	**646**	**9**

***Bold text denotes preferred ages passing discordance.**

DR5 Cathodoluminescence image map of zircon grains from Santo igneous rocks